MIOCENE EVOLUTION OF THE WESTERN EDGE OF THE NEVADA-PLANO IN THE CENTRAL AND NORTHERN SIERRA NEVADA: PALEOCANYONS, MAGMATISM, AND STRUCTURE

Cathy J. Busby[1], Keith Putirka[2]

[1]Department of Earth Science, University of California, Santa Barbara, California 93106, USA

[2]Department of Earth and Environmental Sciences, California State University-Fresno, 2345 San Ramon Ave., MS/MH24, Fresno, California 93720, USA

ABSTRACT

The Sierra Nevada of California is the longest, tallest mountain range in the co-terminus U.S., and has long been regarded as very young (< 6 Ma); however, recent work has provided evidence that the range is very old (> 80 Ma), and represents the western shoulder of a Tibetan-like plateau (the "Nevada-Plano") that was centered over Nevada. A great deal of effort has been invested in applying modern laboratory and geophysical techniques to understanding the Sierra Nevada, yet some of the most unambiguous constraints on Sierran landscape evolution are derived from field studies of dateable Cenozoic strata preserved in paleochannels/paleocanyons that crossed the Sierra Nevada in Cenozoic time. Our work in the Sierra Nevada suggests that neither end-member model is correct for the debate regarding youth vs. antiquity of the range. Many features of the Cenozoic paleocanyons and paleochannels reflect the shape of the Cretaceous orogen, but we suggest that they were also affected by Miocene tectonic and magmatic events.

In the central Sierra Nevada, we infer that the inherited Cretaceous landscape was modified by three Miocene tectonic events, each followed by ~2 – 5 million years of subduction magmatism and sedimentation during a period of relative tectonic quiscense.

The first event, at about 16 Ma, corresponds to the westward sweep of the Ancestral Cascades arc front into the Sierra Nevada and adjacent western Nevada. We suggest that this caused thermal uplift and extension. The second event, at about 11 - 10 Ma, records the birth of the "future plate boundary" by transtensional faulting and

voluminous high-K volcanism at the western edge of the Walker Lane belt. The third event, at about 8 - 7 Ma, is associated with renewed range-front faulting in the central Sierra, and rejuvenation and beheading of paleocanyons. We show that volcanic pulses closely followed all three events, and tentatively infer that footwall uplift of the Sierra Nevada occurred during all three events. By analogy with the ~11 Ma event, we speculate that high-K volcanic rocks in the southern part of the range mark the inception of yet a fourth pulse of range front faulting, at 3-3.5 Ma, that resulted in a fourth tilting and crestal uplift event.

Cenozoic rocks along the western edge of the "Nevada-Plano" record the following variation, from the central to the northern Sierra: decrease in crustal thickness (and presumably paleo-elevation), decrease in paleo-relief and attendant decrease in coarse-grained fluvial and mass wasting deposits, and greater degree of encroachment by Walker Lane-related faults beginning at 10 – 11 Ma. **By mapping and dating Cenozoic strata in detail, we show that what is now the Sierra Nevada was at least in part shaped by Miocene structural and magmatic events.

INTRODUCTION

Great controversy abounds regarding the age and uplift history of the longest and tallest mountain chain in the co-terminus United States. The Sierra Nevada (Fig. 1) has long been considered one of the youngest ranges in North America (< 3 – 6 Ma), formed through uplift of a rigid block about faults along its eastern margin (Whitney, 1880; Lindgren, 1911; Ransome, 1989; Bateman and Warhaftig, 1966; Hamilton and Myers, 1966; Huber, 1981; Unruh, 1991; Wakabayashi et al., 2001). More recent papers have proposed a more complex uplift history for the range, and some have argued for the antiquity of the range (> 80 Ma) (Wolfe et al., 1997; House et al., 1998; House et al., 2001; Horton et al., 2004; Stock et al., 2004; Clark et al., 2005; Cecil et al., 2006; Mulch et al., 2006). Evidence for significant late Cenozoic surface uplift includes tilting of Tertiary sedimentary units and river incision patterns (Christensen, 1966; Huber, 1981; Unruh, 1991; Wakabayahsi and Sawyer, 2001; Jones et al., 2004). However, recent studies have mainly used laboratory techniques to infer that the range has been a longstanding topographic feature of the landscape in the western U.S., including stable isotope studies (Poage and Chamberlain, 2002; Horton et al., 2004; Horton and Chamberlain, 2006; Mulch et al., 2006); thermochronology (House et al., 1998, 2001; Clark et al., 2005; Cecil et al., 2006; Mahéo et al., 2009); cosmogenic nuclide studies (Stock et al., 2005); paleobotanical studies (Wolfe et al., 1997); dating of cave sediments (Stock et al., 2004); and hydrogen isotope studies of widespread ash-fall deposits (Mulch et al., 2008). Some workers, however, have proposed a more intermediate model, wherein a Cretaceous to Eocene inherited landscape surface began to undergo erosional rejuvenation sometime after 20 Ma (Clark et al., 2005; Clark and Farley, 2007; Pelletier, 2007), in response to the inception of the Sierra Nevada microplate (Saleeby et al., 2009; Mahéo et al., 2009). It is also clear that in the southern Sierra, a phase of accelerated river incision began at ca. 3 Ma, in response to > 1 km crestal uplift driven by underlying mantle lithosphere foundering (Ducea and Saleeby, 1996, 1998; Saleeby and Foster, 2004; Zandt et al., 2004; Jones et al., 2004; Saleeby et al., 2009).

In this paper, we interpret new field and geochronological results gathered by us and our students over the past five years, on Cenozoic strata and intrusions in the central and northern Sierra Nevada (Fig. 2, 3, 4, 5, 6, 7; Table 1; Roullet, 2006; Busby et al., 2008a, 2008b; Garrison et al., 2008; Hagan et al., 2009; Koerner et al., 2009; Gorny et al., 2009). These results provide a sensitive record of surface processes over the past ~ 50 m.y., including:

(1) canyons and channels cut by ancient rivers whose lengths, gradients and sedimentological characteristics were controlled by regional-scale elevation and topographic relief,

(2) evidence for long (ca. 2 – 10 my) periods of steady volcano-sedimentary aggradation that alternated with shorter periods of erosion and development of regional-scale unconformities,

(3) an array of volcanic center types, with distinctive eruptive styles, reflecting regional variation in lithospheric thickness, extensional vs. transtensional styles of faulting, and hot spot vs. subduction vs. continental rift magmatism.

(4) Miocene episodes of faulting along the present-day range front and adjacent parts of Nevada to the east, recognized through detailed mapping of dateable volcanic strata. These episodes appear to be synchronous with the development of unconformities.

We offer a new model for the Cenozoic history of the central Sierra Nevada, where channels/canyons that were carved during Cretaceous to Paleocene uplift (referred to here as unconformity 1) were re-incised three times during the Miocene (unconformities 2, 3 and 4), each in response to a tectonic event that immediately preceded a major pulse of magmatism (Fig. 7). We present arguments for a fundamentally tectonic control on the development of the Miocene unconformities.

Another controversy related to the timing of uplift of the Sierra Nevada is the circumstances surrounding the birth of the future plate boundary, which extends from the Gulf of California northward through the Eastern California Shear Zone – Walker Lane belt (Fig. 1). This fault zone forms the transtensional eastern boundary between the Sierra Nevada microplate and the Basin and Range to the east (Fig. 5; Argus and Gordon, 1991; Dixon et al., 2000; Sella et al., 2002), and currently accommodates 20 – 25% of the plate motion between the Pacific and North American plates (Bennett et al., 1999; Thatcher et al., 1999; Dixon et al., 2000; Oldow et al., 2000; Unruh et al., 2003). Recent field and geochronological studies in the Sierra Nevada show that this process began at 10 Ma, with the outpouring of voluminous, geochemically distinctive volcanic rocks, preceded by range-front transtensional faulting and probable uplift (Busby et al., 2008b).

OLD VS. YOUNG MOUNTAIN RANGE: MAGMATIC AND TECTONIC EVENTS

The long-accepted model for the origin of the Sierra Nevada involves uplift of the range through tilting of a block bounded on the east by the westernmost and youngest fault zone of the Basin and Range extensional province, less than 6 m.y. ago (Hamilton and Myers, 1966) (Fig. 3). In contrast, recent papers have proposed that the Sierra Nevada formed along the western shoulder of a high, Tibetan-style plateau centered over Nevada at about 80 m.y. ago, and that extension has caused Cenozoic basins to drop down from high elevations, with the Sierra Nevada and other ranges forming relict highs that have not been uplifted significantly in the Cenozoic (House et al., 1998) (Fig. 3). It is generally agreed that this high plateau or broad altiplano was formed by shortening and crustal thickening due to Cretaceous low-angle subduction beneath the continental margin (DeCelles, 2004; Fig. 3A). There is general agreement that during Cretaceous to Paleocene time, the Cretaceous arc was unroofed to batholithic levels (Cecil et al., 2003) and "paleochannels" or "paleo-canyons" were carved into it, and filled with Eocene to Miocene strata (Lindgren, 1911; Ransome, 1898; Bateman and Warhaftig, 1966; Garside et al., 2005; Busby et al., 2008a, 2008b).

The timing and cause of subsequent Cenozoic extension of this plateau remains controversial. Some workers infer that extension accompanied the southwestward sweep of arc magmatism as the subducting slab fell back to steeper depths during Eocene to Miocene time (Gans et al., 1989; Axen et al., 1993) (Fig. 1). Stable isotope studies on paleosol carbonates, authigenic minerals and metamorphic minerals in normal faults have been used to infer that this southward sweep of arc magmatism and extension was accompanied by an increase in surface elevation, in places estimated at 2.5 to 3.5 km; this is consistent with models for thermal reorganization of the crust and lithosphere during removal of the Farallon slab, or delamination of the mantle lithosphere (Kent-Corson et al., 2006; Horton and Chamberlain, 2006; Mulch et al., 2007).

Our new age and geochemical data on 16 - 6 Ma subduction-related volcanic rocks in the central and northern Sierra, compiled here (Table 1), are consistent with Dickinson's (2007) reconstructions for westward sweep of the arc into that region and coeval subduction off California (Sierra Nevada Ancestral Cascades arc, Figure 1; Putirka and Busby, 2007; Busby et al., 2008b). We attribute the scarcity of subduction-related volcanic rocks and intrusions in the southern Sierra to a southward increase in thickness of the crust that underlay the Sierra Nevada Ancestral Cascades arc, and not to a lack of subduction at that latitude (Putirka and Busby, 2007). We suggest below that uplift and extension not only accompanied southwestward sweep of magmatism through the Basin and Range, but also accompanied extension and emplacement of volcanic rocks in the Sierra Nevada.

We also summarize here data that demonstrate disruption of the western edge of the Nevada-Plano as it began to calve off onto the Sierra Nevada microplate. As discussed by Saleeby et al. (2009), the eastern Sierran escarpment system and the Garlock transform fault serve as reasonable approximations to classic plate boundaries, while the western and northern boundaries of the microplate are highly diffuse transpressional and compressional boundaries (respectively) that are unlikely to yield definitive structural evidence for the timing of microplate inception. The data summarized here support the interpretation that this process began at 11 Ma.

This paper is not intended as a review of all previous lab-based work on the landscape evolution of the Sierra Nevada; instead, it focuses on the stratigraphic record of the paleochannels/paleochannel fills, as well as age patterns of associated intrusions, and attempts to reconcile these data with seemingly contradictory laboratory and seismic data. This paper does not discuss the Cenozoic evolution of the southern Sierra Nevada, partly because paleocanyons have not been resolved there (Saleeby et al., 2009), but largely because that segment has a Cenozoic history that is distinctly different from the rest of the Sierra Nevada; for a full discussion with references, see Saleeby et al., (2009, this volume). This paper presents a new reconstruction of the evolution of the central to northern Sierra Nevada (Fig. 7), using Cenozoic volcanic and volcaniclastic strata that are largely preserved in paleochannels (Fig. 2). We then interpret these paleochannels in the larger context of Cretaceous to Cenozoic landscape evolution of the western U.S.

PALEOCHANNELS, FAULTS AND ANCESTRAL CASCADES ARC VOLCANISM, CENTRAL AND NORTHERN SIERRA NEVADA

Paleochannels of the Sierra Nevada generally trend E-W (Figure 2) and material in them was transported from east to west, as in the modern drainages (Whitney, 1880; Lindgren, 1911; Ransome, 1898; Wakabayashi et al., 2001; Bateman anad Warhaftig, 1966; Garside et al., 2005; Busby et al., 2008a, 2008b; Henry, 2008). These paleo-channels are much better preserved and exposed in the Sierra Nevada than they are in the Basin and Range to the east (Fig. 2), due to disruption by faults and burial beneath basins there. Thus, Sierran paleochannels provide the best opportunity to understand the paleogeography of the western flank of the “Nevada-Plano” (De Celles, 2004?).

In this paper we synthesize newly-published mapping and $^{40}Ar/^{39}Ar$ dating of paleochannel fill in the northern and central Sierra Nevada (Busby et al., 2008a, 2008b;

Garrison et al., 2008; Koerner et al., 2009; Hagan et al., 2009) (Fig. 4) to define these magmatic and inferred tectonic events (Fig. 7): ~ 16 Ma flood basalt volcanism and weak extension in the northern Sierra, and three distinct episodes of Miocene faulting and possible uplift in the central Sierra: at about 16 Ma, at 11 Ma, and at 8 - 7 Ma. Each of the three postulated Miocene uplift events are recognized by an erosional unconformity that has been mapped out along the axes of paleocanyons, and correlate between paleocanyons of the Central Sierra (Busby et al., 2008a, 2008b; Hagan et al., 2009). We refer to the unconformity between granitic bedrock and the Oligocene ignimbrites as unconformity 1, and the three Miocene unconformities as unconformities 2 through 4 (Fig. 7; Hagan et al., 2009). Minor erosional surfaces locally occur between these unconformities but those cannot be traced any distance. For example, two unconformities in the modern Kirkwood Valley (unconformities 4 and 5 of Busby et al. (2008a) could not be correlated to other paleocanyons (Busby et al., 2008b), and are now known to merge with up-paleocanyon with unconformity 3 of this paper (Hagan et al., 2009). Each of the three inferred Miocene uplift events were separated by longer periods of aggradation of arc volcanic and sedimentary rocks, with no evidence of reincision in the paleocanyons (Fig. 7). This aggradation produced unconformity-bounded sequences, which are given the number of the unconformity that underlies them, as is customary (see references in Busby and Bassett, 2007). Thus, in the central Sierra, sequence 1 consists of the basal Oligocene ignimbrites, which rest upon on granitic basement. Sequences 2, 3 and 4 consists of Miocene volcanic and volcaniclastic rocks that are ~ 16 - 11 Ma (Middle Miocene), ~ 10 - 8 Ma (early Late Miocene), and 7 – 6 Ma (late Late Miocene) in age, respectively. Work in progress will more closely define the ages of unconformities and sequences.

In this section we use a time slice approach to describe and interpret key features of the mapped and dated unconformities and sequences. We also describe any direct or indirect links we can make between the development of unconformities and faulting in the region. In the following section, we discuss possible alternative explanations for the development of the unconformities (e.g. changes in climate, sediment supply, etc.) and explain why we prefer a tectonic explanation for their origin.

Oligocene – Early Miocene Ignimbrites in Paleochannels Inherited from Cretaceous – Paleocene Time (Sequence 1)

Eocene sedimentary rocks that constitute the basal fill of paleochannels cut into Cretaceous granitic basement of the Sierra Nevada have yielded indefinite results concerning the paleogeography of the range (Cecil et al., 2006). These are mainly preserved in paleochannels of the northern Sierra, and not present in the central high Sierran paleocanyons described here.

Much more clear are the implications of the presence of ~ 22 – 30 Ma ignimbrites in the paleochannels (Fig. 7, cross section 1). These ignimbrites erupted from calderas situated in central Nevada (Garside et al., 2005; Henry, 2008) (Fig. 2). For these to have flowed from central Nevada to the Sacramento Valley of central California, surface elevations must have continuously decreased in that direction, and the region could not have yet been disrupted by normal faults.

In the central Sierra Nevada, unconformity 1 is an extremely rugged surface, especially where it is cut into metamorphic rocks, which form fins, but also where it is cut into granitic rock, as show in Fig. 6A. In this paper, we refer to the ignimbrites as sequence 1, because they overlie unconformity 1 in the high central Sierra. These ignimbrites generally have small pumices and few, small lithic fragments, consistent with their distal nature (Fig. 6B). Although it is obvious from their mineralogy that several different ignimbrite sheets filled the paleocanyons, we have not attempted to divide them, because they were largely eroded away during the development of unconformity 2 (described below).

Eruption of 16 Ma Flood Basalts Through Incipient Sierran Frontal Fault

The oldest Cenozoic volcanic rock that vented through what is now the Sierra Nevada is a flood basalt erupted from a fissure along the Honey Lake fault zone, in the northern Sierra just west of Honey Lake (Fig. 2, 5). The Lovejoy basalt is the largest known eruptive unit in California, and has geochemical affinities with coeval flood basalts of the Columbia River Group (Fig. 1) (Garrison et al., 2008).

The fissure vent for the Lovejoy basalt lies along one of the most important fault zones of the Walker Lane belt, the Honey Lake fault zone (Figure 7, cross section 2;

Garrison et al., 2008). Unlike other Miocene flood basalts of the western U.S., it was not erupted in a backarc position, but rather at the front of the arc (see 15 – 20 Ma position of the arc front in Figure 2B). The fissure vent basalt magmas lies along the Honey Lake fault zone, suggesting that at least incipient mild extension, and perhaps some normal fault-related footwall uplift, occurred in the northern Sierra at about 16 Ma.

Westward Sweep of Ancestral Cascades Arc Front Into Sierra Nevada at 16 Ma (Sequence 2)

In the central Sierra, ignimbrites that gradually accumulated over a long period (from ~30 to ~22 Ma, Fig. 7, cross section 1) were deeply dissected along unconformity 2 prior to the first pulse of arc volcanism, dated at 16 – 13 Ma (Fig. 4). However, the ignimbrites were not dissected in the northern Sierra (see Fig. 5 of Garside et al., 2005; Busby's unpublished mapping). This difference indicates that climatic change was not the primary control on the unconformity, since that would presumably affect both areas. For reasons given in this section, we infer that the control was thermo-tectonic (Fig. 7, cross section 3).

The Oligocene ignimbrites were virtually reamed out of the central Sierran paleocanyons during the development of unconformity 2, leaving bits of their stratigraphy stranded on paleo-ledges, paleo-walls and parts of the irregular paleocanyon floors. Unconformity 2 is locally overlain by granitic boulder conglomerate (Fig. 6C), suggesting at least local incision into bedrock at this time.

As noted above, recent stable isotope work has shown that the southwestward sweep of the arc through Idaho and Nevada was accompanied by synchronous extension and increase in surface elevation, interpreted to record thermal effects as the Farallon slab fell back (Kent-Corson et al., 2006; Horton and Chamberlain, 2006; Mulch et al., 2007). By analogy, we suggest that unconformity 2 records the same process. We therefore assign an age of ~16 Ma to this inferred uplift event, since that is the age of the westward sweep of the arc into the Sierra Nevada (Fig. 7, cross section 3). More local evidence for the timing of onset of extension (but without evidence for or against synchronous increase in surface elevation) comes from adjacent parts of Nevada. Extension in the Wassuk Range and the Singatse Range (Fig. 5) is estimated to have occurred between about 15 and

14 Ma, and between about 15 and 12 Ma, respectively (Proffett, 1977; Dilles and Gans, 1995; Stockli et al., 2002; Surpluss et al., 2002). This is similar to the age we infer for the development of unconformity 2 in the central Sierra.

The ~16 Ma uplift event was followed by a period of tectonic quiescence in the central Sierra, when ~16 – 13 Ma volcanic rocks (Fig. 4) and ~13 – 11 Ma fluvial and debris flow deposits of sequence 2 aggraded within paleochannels, and no unconformities formed (Fig. 7, cross section 3) (Busby et al., 2008A, 2008B; Hagan et al., 2009). Nonetheless, steep slopes persisted in the central Sierran paleocanyons during accumulation of sequence 2, as shown by the presence of avalanche megablocks (Fig. 6D). Age controls on the first pulse of magmatism in the Sierra are the poorest of the three pulses (Fig. 4) because the oldest volcanic rocks are the most altered, making it harder to find fresh samples suitable for dating (note the larger error on these ages).

Andesitic intrusive, volcanic and volcaniclastic rocks of sequence 2 are not distinguishable from those of sequence 3 and 4 on the basis of any field, petrographic or geochemical characteristics, with the notable exception of the distinctive high-K rocks of the Stanislaus group around Sonora Pass (described in sequence 3, below). Like the rest of the Miocene Ancestral Cascades arc rocks in the Sierra Nevada, sequence 2 includes shallow-level intrusions, block-and-ash-flow tuffs, volcanic debris flow deposits and fluvial deposits, nearly all of andesitic composition; lava flows are rare (Busby et al., 2008b). Petrified wood occurs in debris flow deposits (Fig. 6E) and charred wood occurs in block-and-ash-flow tuffs. Block-and-ash-flow-tuffs are monomict (Fig. 6F), and lack any pumice, indicating an origin by lava dome collapse. These are interstratifed with and pass down-paleocanyon into debris flow deposits, which in turn are interstratified with and pass down-paleocanyon into fluvial deposits (Fig. 6G, 6H, 6I). Well-stratified, well-sorted fluvial deposits with rounded clasts occur at all stratigraphic levels in sequence 2, including the base of the sequence (e.g. see volcanic fluvial conglomerate and sandstone unit Tvf1 of Hagan et al., 2009). This indicates that at least some of the sediment was derived from points east of the present-day Sierra Nevada, so our proposed ~16 Ma thermal uplift/extensional event must not have not disrupted drainages. One important difference between sequences 2, 3 and 4 is that sequences 2 and 3 have a much higher proportion of well-rounded, well-sorted fluvial deposits in what is now the crestal region of the Sierra; as discussed below, we infer that this records Late Miocene beheading of the paleocanyons from sources to the east in Nevada, due to range-front faulting.

Much less is known about rocks of sequence 2 age in the northern Sierra, due to a general lack of detailed maps and dates there, but Garrison et al. (2008) presented a single date of 14 Ma (Table 1) on an andesite lava flow that lies upsection from the Lovejoy basalt at Red Clover Creek (Fig. 5).

Dextral Transtension and High-K Volcanism: Birth of the Sierra Nevada Microplate at 11 Ma (Sequence 3)

Andesite volcanic and volcaniclastic rocks that steadily aggraded in paleochannels from ~16 to ~11 Ma were deeply incised along unconformity 3 before the onset of volcanic pulse 2 (Fig. 7, cross section 4), which spans ~10.7 – 9 Ma (Fig. 4). Sequence 3 includes high-K lava flows and ignimbrites in the Sonora Pass to Ebbetts Pass region, and andesitic volcanic and volcaniclastic rocks in the Ebbetts Pass to Carson Pass region (Busby et al., 2008 a, 2008b; Hagan et al., 2009; and our unpublished mapping). Numerous workers have inferred that the high-K rocks erupted from the Little Walker Caldera, also referred to as the Little Walker Center (Slemmons, 1966; Priest, 1979; Noble et al., 1974, 1976; Putirka and Busby, 2007; King et al., 2007; Busby et al., 2008b; Koerner et al., 2009; Pluhar et al., 2009).

We have direct evidence for the onset of dextral transtensional range-front faulting during the development of unconformity 3, immediately prior to the beginning of eruption of the high-K rocks. Busby et al. (2008b) mapped a series of east-dipping, down-to-the-east normal faults that step right round the Little Walker Center, including (from west to east) the St. Mary's Pass fault, the Leavitt Meadow – Lost Cannon fault, the Grouse Meadow fault, and the Sonora Junction fault (Fig. 5). A 500 m thick avalanche deposit with blocks up to 1.6 km was shed from the footwall of the St. Mary's Pass fault onto its hangingwall within 140 kyr of the beginning of the high-K eruptions, as shown by ages on transported material in the avalanche blocks and on the basal unit of the high-K rocks (Table Mountain Latite lava flows) (Busby et al, 2008b). Chaotically-tilted strata in landside blocks beneath Table Mountain Latite are obvious from Highway 108, including views from Sonora Pass northward toward Sonora Peak (Fig. 6G) and views east of the pass toward the south at Sardine Falls (Fig. 6J). Along the next fault to the east, the Lost Cannon fault (Fig. 5), sequence 1 and 2 strata are rotated much more steeply by the fault than the overlying Table Mountain Latite of sequence 3, and the sequence 2 andesitic volcaniclastic rocks contain avalanche blocks of sequence 1 ignimbrites, indicating that this fault also began to slip prior to eruption of the high-K rocks (Busby et al., 2008b). Additional slip on that fault during eruption of the Table Mountain Latite may be indicated by dramatic thickening of the lavas and interstratified fluvial sandstones toward the fault (Busby et al. 2008b). All of these faults were re-activated after emplacement of sequence 3 volcanic rocks, and some show evidence of Quaternary to Recent displacement; it was only through detailed mapping of the Miocene paleocanyon fill that the 11 Ma initiation of this fault zone could be recognized. We thus infer that the Little Walker Caldera (Fig. 5) was formed along a releasing stepover of this fault zone (Putirka and Busby, 2007; Busby et al., 2008b).

Sequence 3 strata in the Sonora Pass area is dominated by the eruptive products of the Little Walker Center/Caldera. In its earliest activity, it was likely the source for the second largest known lava flow unit in California (after the Lovejoy basalt), the 10.4 Ma Table Mountain Latite (Table 1). The Table Mountain Latite consists of voluminous trachyandesite to trachybasaltic andesite lavas (Putirka and Busby, 20007) that flowed westward through paleochannels in the central Sierra Nevada to the Central Valley (Ransome, 1898; Slemmons, 1953, 1966; Priest, 1979; Noble et al., 1974; King et al., 2007; Gorny et al., 2009; Koerner et al., 2009; Pluhar et al., 2009). Flow within paleo-river channels is indicated by presence of blocky jointing on the tops of some flows (Fig. 6K), suggesting quenching by water, and stretching of vesicles parallel to the trend of the palecanyon system (Fig. 5L). At the present-day Sierran crest, the Table Mountain Latite consists of 23 lava flows and is over 400 m thick (Busby et al., 2008b). In its distal facies, 130 km to the west near Knight's Ferry, it is up to 45 m thick, and consists of one very thick flow and three much thinner flows with weathered tops, which paleomagnetic data show all erupted in less than a few centuries (Gorny et al., 2009). The proximal facies of the Table Mountain Latite section locally has minor olivine basalt lava flows, which are useful for petrogenetic studies (Putirka and Busby, 2007; Koerner et al., 2009; work in progress). The 10.4 Ma Table Mountain Latite is overlain by the 9.54 – 9.34 Ma Eureka

Valley tuff (Table 1), which consists of three trachydacite ignimbrite members (King et al., 2007; Koerner et al., 2009), also erupted from the Little Walker Caldera (Priest, 1979; King et al., 2007). The lower two members of the Eureka Valley Tuff make a very distinctive black ledge across the landscape (Fig. 6M), and also have distinctive black glassy fiamme on outcrop (Fig. 6N). High-K lavas previously recognized between the lower two members of the Eureka Valley Tuff at the caldera (Priest, 1979; Brem, 1984) are also present in the Sierran paleocanyon at Sonora Pass (Koerner et al., 2009). This unit, which we refer to as the Lava Flow Member of the Eureka Valley Tuff, includes both normal- and reversed–polarity lava flows (Pluhar et al., 2009), and ranges from trachyandesite to trachydacite in composition (Koerner et al., 2009). The Dardanelles Formation, which also consists of high-K lavas flows (trachyandesites or shoshonites), has long been inferred to lie above Eureka Valley Tuff (Slemmons, 1966; Noble et al. 1974, 1979) although no maps or measured sections were previously published to demonstrate that it lies above all three members of Eureka Valley Tuff; previous workers have therefore confused it with the Lava Flow Member of the Eureka Valley Tuff or the Table Mountain Latite at some localities (Koerner et al., 2009). New mapping west of Sonora Pass demonstrates that trachyandesite lava flows do in fact overlie the Upper Member of the Eureka Valley Tuff (Koerner et al. 2009). The Dardanelles Formation is not yet dated, but its normal magnetic polarity suggests it was erupted between 9.44 and 9.35 Ma, or else it is younger than 9 Ma (Pluhar et al., 2009). Together, all of these high-K volcanic rocks make up the Stanislaus Group, which we infer records low-degree partial melting of mantle lithosphere along a pull-apart structure. We infer that the eruptive products of the Little Walker Caldera formed in a pull-apart basin bounded by releasing stepover faults that penetrated a lithospheric plate with a thick crustal section. These transtensional stresses resulted in the eruption of low degree (high-K) partial melts (Putirka and Busby, 2007) (Fig. 7, cross section 4), signaling the birth of the Sierra Nevada microplate (Fig. 1). This ~ 10.5 Ma faulting clearly did not succeed in completely disrupting the paleocanyon system, because the 10.4 – 9 Ma eruptive products were funneled along it.

Unlike the Sonora Pass to Ebbetts Pass area, we cannot demonstrate a direct link between faulting and development of unconformity 3 in the Carson Pass area (Hagan et al., 2009). However, just to the east in the Gardnerville basin (Fig. 5), gravity studies show evidence for older (pre-7 Ma) normal faults buried beneath the 7 Ma – Recent basin fill associated with the Genoa fault (Cashman et al., 2009). Perhaps these faults also record the birth of the Sierra Nevada microplate. There is no evidence for high-K volcanism in sequence 3 strata between Ebbetts Pass and Carson Pass. Instead, these strata consist largely of andesitic volcaniclastic debris and fluvial deposits reworked down-paleocanyon from sources to the east, indicating that the paleocanyon system was not yet completely disrupted by faults. In addition, sequence 3 strata at Carson Pass contain proximal volcanic rocks including block-and-ash-flow tuffs and peperitic intrusions (Busby et al. 2008a; Hagan et al., 2009).

We tentatively suggest that 11-10 Ma initiation of the Sierra Nevada microplate is recorded in the Cenozoic strata of the northern Sierra (as well as the central Sierra). Miocene rocks there have not been mapped in great detail, although a series of 1:62,500 and 1:100,000 maps are available from the California Geological Survey (Grose et al., 1990; Grose and Mergner, 2000; Grose, 2000a, 2000b, 2000c, 2000d) and are very useful for selecting key areas suitable for more detailed work. On the basis of more detailed (1:24,000 scale) mapping, we have preliminary evidence that the northern Sierra began to be broken into the structural blocks that define the northeastern boundary of the Sierra Nevada microplate at 11 – 10 Ma. Unpublished detailed mapping and dating of the Dixie Mountain center area (Fig. 5; Roullet, 2006) and unpublished reconnaissance mapping by Busby indicates that a section of andesitic volcanic debris flows, lesser block-and-ash-flow tuffs, and minor lava flows at least 500 m thick covers an area of at least 20 X 30 km. This section accumulated in less than 0.3 myr (between 10.8 and 10.5 Ma Ma, Table 1), which is a very high rate (1.6 mm/yr). We tentatively propose that this section was accommodated by subsidence of an intra-arc basin that formed between the Mohawk Valley and Honey Lake fault zones (Fig. 5), although further mapping and dating are needed to better define this basin. The basin may thus record the beginning of dismemberment of what is now the northern Sierra along the northern boundary of the Sierra Nevada microplate. The Dixie Mountain center, which intrudes this basin fill, is a 10.5 Ma laccolith that was emplaced mainly at the contact between the granitic basement and the volcaniclastic basin fill, and warped the fill upward off the basement. However, the laccolith also intruded up through the basin fill as a series of sills, “Christmas tree” style, and it locally broke through the cover to vent block-and-ash flows into the basin(Roulett, 2006; Busby et al., unpublished data). Intrusions of the Dixie Mountain center extend about 13 km in a NNW-SSE direction and about 9 km in a WSW-NE direction, suggesting a structural control on its position and shape.

An ~10 - 11 Ma age for the birth of the Sierran microplate is supported by studies from many other parts of the Sierra Nevada and adjacent regions. On the north side of present-day Lake Tahoe (Fig. 1), the Verdi-Boca basin formed at ~12 Ma, along the down-to-the-east Donner Pass fault (Henry and Perkins, 2001). This fault forms part of the Tahoe-Sierra frontal fault zone of Schweickert et al. (1999, 2000, 2004), which runs up the west side of Lake Tahoe. Across Lake Tahoe to the east in the Carson Range, Tertiary strata useful for determining direction and timing of tilting are rare, but Surpless et al. (2002) modeled thermochronological data to infer a 15 degree westward tilting of the Carson Range, at about 10 to 3 Ma. In the southern Sierra Nevada, He apatite data from the footwall of the Mount Whitney escarpment indicate rapid tectonic denudation at ~ 10 Ma (Mahéo et al., 2004). The Indian Wells segment of the eastern escarpment of the southern Sierra Nevada shed sediment into the El Paso basin by ~ 8 Ma (Loomis and Burbank, 1988). Finally, a massive sand sheet in the San Joaquin basin records an ~ 10 Ma phase of uplift and incision of southern Sierran granitic basement (Saleeby et al., 2009); in contrast, basement incision in the central to northern Sierra basement was delayed until Pliocene time. As discussed below, we infer that it was delayed there because base level in the adjacent Great Valley was raised dramatically by the production of a volcaniclastic fluvial wedge. Saleeby et al. (2009) infer that the ~ 10 Ma event resulted in westward tilting and uplift that was to a first order uniform along the length of the microplate, producing an elevation increase of ~1,000 m along the eastern Sierra crest. We argue below that this fundamental, plate margin-scale event is what produced unconformity 3, rather than other possible controls, such as fluctuations in sediment supply or climate.

Renewed Extension, Rejuvenation and Beheading of Paleocanyons, and 7 – 6 Ma Volcanism (Sequence 4)

Our age constraints on the timespan covered by unconformity 4 are as follows: It cuts the ~10.5 to 9 Ma volcanic rocks, and is overlain by volcanic rocks as old as 7 Ma (Busby et al., 2008a). However, in the Ebbetts Pass area, the 9 Ma rocks are overlain by a thick, undated section of andesitic fluvial and debris flow deposits (Keith et al., 1982), so we prefer the interpretation that the unconformity formed between 7 and 8 Ma. We infer that unconformity 4 records renewed range-front faulting (and possible footwall uplift) at about 7 – 8 Ma (Fig. 7, cross section 5).

Range-front faults clearly controlled the positions of volcanic centers during magmatic pulse 3. One of the bigger volcanic centers recognized in the Sierra, the Markleeville Center, developed within the Hope Valley graben at Carson Pass at this time (CP, Fig. 2). This center is about 8 km in diameter and consists of hornblende dacite and andesite intrusions and altered roof rocks (Hagan et al., 2009). Sequence 4 andesite lava flows also erupted along this fault zone, and andesites intruded fault breccias in the granitic basement (Hagan et al., 2009). The next fault to the east of the Hope Valley graben, which we name the Grover Hot Springs fault (Hagan and Busby, unpublished mapping), extends southward to Ebbetts Pass (Armin et al, 1984), where it overlaps with the Noble Canyon fault of Armin et al. (1984) (Fig. 5). Activity on the Grover Hot Springs and Noble Canyon fault overlapped in time as well as space (Hagan and Busby, unpublished mapping). Immediately south of the area of fault overlap, in the Ebbetts Pass paleocanyon, lies a landslide deposit several hundred meters thick, composed of andesitic strata. This landslide deposit was shed from the area of fault overlap, due to tilting along the lateral ramp, because granitic basement rocks and sequence 1 Oligocene ignimbrites are exhumed and Miocene arc strata are missing on the ramp. This exhumed basement thus forms part of unconformity 4. The ramp then acted as a sediment transfer path for granitic boulders that were funneled into sequence 4 strata of the Ebbetts Pass paleocanyon (Fig. 6O). Sequence 4 breccias at Ebbetts Pass are the coarsest in the central Sierran paleocanyons (Fig. 6P). The Grover Hot Springs fault (and a shorter fault to the east of it, the Silver Mountain fault, Fig. 5) controlled the siting of a 10 km diameter volcano, which we call the Ebbetts Pass center (Hagan and Busby, unpublished mapping). This volcano consists of radially-dipping basaltic andesite lava flows, with a dacitic intrusive core that sits directly above the projected trace of the Grover Hot Springs fault

(Fig. 6Q; Hagan, Busby, Putirka and Renne, unpublished mapping, geochemistry and dating in progress). Although this volcano is not yet dated, map relations suggest that it forms part of the 7-6 Ma magmatic pulse (sequence 4). The Nobel Canyon fault shows evidence of minor reactivation after the volcano formed, because it offsets the western margin of the volcano by about 100 m. (Hagan and Busby, unpublished mapping).

Unconformity 4 is the deepest and steepest-sided Miocene unconformity in the central Sierra. In places it downcut into granitic basement, and it formed local slopes of up to 48 degrees, representing very steep paleo-canyon walls in the late Late Miocene. Mass wasting deposits are common in sequence 4, and include slide and avalanche blocks hundreds of meters in size (Skilling et al., 2009). Some of the larger slide blocks consist of lithified sequence 3 debris flow deposits complete with their 10 – 11 Ma andesitic intrusions, described *in situ* by Busby et al. (2008a) and Hagan et al. (2009). These steep-sided canyons prone to mass failure were more like gullies than channels, because they served less as fluvial conduits than as depocenters for locally-sourced breccias, debris flow deposits, lava flows and block-and-ash-flow tuffs. Sequence 4 lacks the andesitic fluvial sandstones and conglomerates that occur at all stratigraphic levels in the other Miocene sequences (2 and 3). We interpret this to mean that the paleocanyons were beheaded by the range-front faults by this time.

Post-Miocene Faulting

Some of the faults that we infer were active during the development of unconformities 2, 3 and 4 were clearly reactivated at some time after arc volcanism ceased at ~ 6 Ma due to passage of the triple junction (Fig. 1), since they offset the youngest volcanic deposits. Some remain active today; for example, the Sonora Junction fault (Fig. 5) has fresh scarps along it. Similarly, the Genoa fault (Fig. 5), which has active seismicity, began to slip at 7 Ma (Cashman, 2009). It is not known whether the range-front zone remained continuously active, or moved episodically between 6 Ma and present. However the deposits of sequence 4 are cut by the modern canyons of the Sierra Nevada, so faulting and tilting have occurred since Miocene time.

SIGNIFICANCE OF UNCONFORMITIES

We recognize three Miocene unconformities, 300 – 600 m deep (vertical distance from top to bottom), in the central Sierra Nevada. These are too deep to be the result of eustatic base-level changes, so they must record changes in climate or sediment supply, or have fundamentally tectonic controls.

Existing climate data from the western U.S. do not suggest any dramatic changes that could easily explain the unconformities. Horton and Chamberlain (2006) instead suggest that gradual climate change occurred, in the form of prolonged cooling and aridification since the middle Miocene, consistent with marine climate records that indicate a ~5 degree centigrade drop in temperature. They also discounted the importance of any paleo-latitudinal changes on climate, because the western U.S. has been at about the same latitude throughout the Cenozoic (Horton and Chamberlain, 2006). Furthermore, Mulch et al. (2008) have recently used hydrogen isotope data on hydrated glasses to infer that climate and precipitation patterns have not changed substantially over the last 12 million years or more. Last, as argued above, it seems unlikely that climate change was the main control on the erosion of unconformity 2, because it is very strongly developed in the central Sierra, and is virtually absent in the northern Sierra; a change in climate would have presumably affected both areas.

One possibility invoked for the origin of unconformities in other volcanic terranes is eruption-induced aggradation, in the form of catastrophic sedimentation triggered by explosive eruptions, followed by dissection to base level when the explosive volcanism ends (Smith and Lowe, 1991). The paleochannel fill of the central Sierra Nevada does not fit this model for two reasons: (1) The aggradation-reincision events predicted by an eruption-induced mechanism occur on a short time scale (that of the activity and dormancy of a volcano, which is typically much less than 10 kyr in arc volcanoes), and are dominated by explosive volcanic products. Although the Oligocene to Early Miocene aggradational event was fed from explosive eruptions, aggradation was ongoing for ~ 8 my before dissection began in the central Sierra. (2) The paleochannel fill for the younger two (Miocene) aggradation events lacks explosive volcanic products, and although some of its fill is catastrophic in nature (lava flows, debris flows), much of its fill is non-catastrophic in nature (fluvial conglomerate and sandstone), with sedimentary structures that suggest steady, prolonged aggradation. These aggradational events spanned ~ 5 my to ~ 2.5 my.

It has been argued that the only unconformity that can be used to infer Cenozoic uplift of the Sierra Nevada is the post-5 Ma unconformity, because that is the only one that incises through Cenozoic strata into basement rocks (Wakabayahsi et al., 2001). This interpretation makes the assumption that base level (the lowest point to which a stream can flow) has been the same for Sierran rivers ever since Cretaceous or Paleocene time. This is a reasonable assumption for periods of time when Sierran rivers had their mouths at the sea, as recorded in the marine Eocene Ione Formation of the westernmost Sierra Nevada foothills. However, Oligocene and Miocene rivers of the northern and central Sierra north of latitude 37° debouched into a nonmarine basin in the California Central Valley (Repenning, 1960; Bartow, 1991). We infer that base level rose in the Central Valley in Oligocene to Early Miocene time, due to transport of voluminous volcaniclastic sediment through paleochannels from volcanoes in western Nevada, before the ~ 16 Ma uplift event occurred in the central Sierra Nevada. Furthermore, we suggest that base level continued to rise as even more voluminous volcaniclastic sediment was supplied to the channels from Ancestral Cascades arc volcanoes in the northern and central Sierra Nevada, during the time that the next two uplift events occurred (at ~11 Ma and at ~ 8 Ma). We suggest that the nonmarine volcaniclastic wedge backfilled the lower reaches of the paleocanyons and spread across the foothills, raising base level by hundreds of meters. This model could be tested through apatite He dating on the granitic basement, to look for age patterns indicative of differential disturbance due to thermal blanketing by sediment burial (Shuster et al., 2006; Flowers et al., 2007), similar to that found in the southern Sierra by Mahéo et al. (2009).

If the unconformities simply record re-incision after a canyon has been filled, we see no reason why the unconformities should be the same age from paleocanyon to paleocanyon, since different materials were supplied to different paleocanyons at different times, and downcutting through a lava flow should take a great deal longer than downcutting through unlithified sands or gravels. Similarly, if incision occurred in response to a change in sediment flux, the timing of this should vary from paleocanyon to paleocanyon, because of the rapidly shifting nature of volcanic activity in the headwaters of the paleocanyons. Thus, we consider it most likely that the unconformities formed in response to coeval episodes of Miocene faulting, which we have clear evidence for, and we infer that footwall uplift produced the unconformities. This is consistent with the surface process modeling results of Pelletier (2007), which identifies two major pulses of surface uplift for the Sierra Nevada: one in the latest Cretaceous, and one in the Miocene (~ 15 - 10 Ma).

THE SHAPE OF THE CRETACEOUS HIGH PLATEAU AND ITS INFLUENCE ON CENOZOIC LANDSCAPE EVOLUTION

We have previously inferred that a north-to-south decrease in Ancestral Cascades arc volcanic rocks (Fig. 1) and concomitant increase in potassium content of these magmas in the Sierra Nevada were controlled by a marked north-to-south increase in thickness of low-density crust, which is reflected in a southward increase in present-day summit elevations (Putirka and Busby, 2007). Consistent with this interpretation are our findings that: (1) paleo-relief, defined as relief that pre-dates Cenozoic deposits, increases southward within the range (Wakabayashi et al. 2001; Bateman and Warhaftig, 1966; Busby et al., 2008a), (2) the paleochannels in the northern Sierra are broader and more flat-floored than the paleocanyons in the central Sierra, which locally show slopes up to 50° on granitic basement (Busby et al., 2008a), (3) the unconformities produced by Miocene re-incision events in paleochannels of the northern Sierra are less than 15m deep (vertical distance of erosion), even though the deposits are of similar thickness to the ones in the central Sierra (Wakabayashi et al. 2001), while in the central Sierra paleocanyons the Miocene unconformities are ~ 400 – 600 m deep (Busby et al., 2008a, 2008; Hagan et al. 2009), and (4) fluvial deposits in the central Sierran paleocanyons are much coarser than they are in the northern Sierran paleochannels, indicating higher axial gradients; also, mass wasting deposits, which are common in central Sierran paleocanyons, have not been reported from northern Sierran paleochannels.

North of the northern Sierra Nevada, voluminous Late Cretaceous batholith rocks curve eastward into northwest Nevada (Fig. 1), where the crust was extended only a minor amount (<15 - 20%), and is relatively thin (Lerch et al., 2008). Like the northern Sierra, Miocene volcanic-volcaniclastic strata in northwest Nevada are widespread, in contrast to the central Sierra where volcanic strata are preserved in paleochannels; this indicates low paleo-relief.

Taken together, field and geochemical data suggest that that the edge of the Cretaceous "Nevadaplano" (DeCelles, 2004) decreased in elevation northward between the central and northern Sierra, and that its edge curved northeastward through northwest Nevada. Thus, the highest part of the "Nevadaplano" corresponds in part to the region of large-magnitude (~100%) Cenozoic synvolcanic extension, although it was broader, reaching northward as far as Reno (Fig. 1) (Gans et al., 1989; Axen et al., 1993; Dickinson, 2007), with an areal extent that was possibly controlled by the paleo-edge of the North American continent. Sediment eroded off the high plateau may have drained northward as well as westward, into the Hornbrook basin of southeastern Oregon as well as the Central Valley of California (Fig. 1). The north-draining paleochannels, if they exist, are covered by Pliocene to Recent Cascades arc volcanic rocks, with the possible exception of the "Jura River", described in Lindgren's classic 1911 study as a northward-draining paleochannel in the northern Sierra (Fig. 2) (Lindgren, 1911). Lindgren contrasted the fine-grained deposits of this river, sand and lignite, with the coarser fill of the west-flowing paleochannels. This is consistent with our view that the Central Sierran features are more aptly termed "paleocanyons" for their ruggedness, deep unconformities and coarse fill (Busby et al., 2008a), while the northern Sierran paleochannels developed on gentler slopes.

CONCLUSIONS

A great deal of effort has been invested in applying modern laboratory and geophysical techniques to understanding the Sierra Nevada, yet some of our most unambiguous constraints on Sierran landscape evolution derive from field studies of Cenozoic strata. New geologic data constrain the timing and nature of magmatic and sedimentary events, faulting, and possible uplift, thus providing a new and important context for laboratory and geophysical studies.

Geologic work in the Sierra Nevada shows that neither end-member model is correct for the debate regarding youth vs. antiquity of the range. Many features of the

Cenozoic paleocanyons and paleochannels reflect the shape of the Cretaceous orogen (unconformity 1), but they were also affected by Miocene tectonic and magmatic events, (in addition to Pliocene to Recent events, not discussed here). In the central Sierra Nevada, we infer that faulting and possible uplift immediately preceded three arc volcanic pulses (at about 16, 11 and 8 Ma). These Miocene uplift events did not produce unconformities that cut down below the Cretaceous-Paleocene unconformity, because base level was raised in the Central Valley by the construction of a very thick nonmarine volcaniclastic wedge.

The fill of the paleocanyons (where they have been studied in detail, near the present-day Sierran crest) records the progressive dismemberment of the Nevada-Plano and, ultimately, canyon beheading. Sequence 1 is composed entirely of material (Oligocene ignimbrite) sourced from the highest part of the Nevada-Plano. This material gradually filled the paleocanyons over about ten million years. Sequences 2 and 3 (early and middle Late Miocene) contain a mixture of vent-proximal volcanic rocks and fluvial sediment derived from more distant sources, presumably in Nevada. Sequence 4 (late Late Miocene) is floored by a rugged, deep unconformity, and lacks fluvial sediment derived from more distal sources; it records rejuvenation of the paleo-canyons, presumably by crestal uplift along range-front faults, and their beheading.

While detailed mapping and dating are still in progress, we tentatively offer the following model for the Miocene structural evolution of the central to northern Sierra Nevada range:

1. Regional normal faulting at about 16-15 Ma was synchronous with development of unconformity 2, followed by the onset of arc volcanism. Although we have not yet identified normal faults of this age along the Sierra Nevada range front, the incipient Honey Lake fault zone controlled the emplacement of basalt fissures in the northern Sierra at this time, and normal faults of similar age have been dated in some of the ranges immediately to the east of the central Sierra. We would expect this extension to have covered a relatively broad area but perhaps be the weakest of the three Miocene events, if it was associated with stretching over a region of thermal uplift.

2. Regional range-front faulting at 11 Ma occurred synchronously with the development of unconformity 3, followed immediately by high-K volcanism. This records

the birth of the “future plate boundary” along the east margin of the Sierra Nevada microplate. This plate boundary was born in the axis of the ancestral Cascades arc along the central Sierran range front faults, during large-volume, high-K eruptions at the Little Walker caldera (Putirka and Busby, 2007; Busby et al., 2008b). The 11 Ma event was a plate-margin-scale event.

3. Range-front faulting resumed at about 8-7 Ma, synchronous with the development of unconformity 4. These faults controlled the siting of volcanoes, and some faults were re-activated to offset the volcanoes.

By analogy with the ~11 Ma event, we speculate that high-K volcanic rocks in the southern part of the range mark the inception of yet a fourth pulse of range front faulting, at 3-3.5 Ma.

Our data from the central Sierra show that each of these range-front faulting episodes was synchronous with the development of an unconformity in the paleocanyons, and was closely followed by emplacement of Ancestral Cascades arc intrusions and volcanic rocks. We therefore consider these events related, and infer a primarily tectonic control on the development of the unconformities.

Whether or not the interpretation of a fundamentally tectonic control on the unconformities is accepted by future workers, we have clearly shown that the Sierra Nevada cannot be regarded as a passive shoulder to the Nevada Plano in Miocene time. By mapping and dating Cenozoic strata in detail, we have shown that what is now the Sierra Nevada was partly shaped by Miocene structural and magmatic events. That must be taken into consideration in any models put forward for the origin of the range.

ACKNOWLEDGMENTS

This research was supported by National Science Foundation grant EAR-01252 (to Busby, Gans and Skilling), EAR- 0711276 (to Putirka and Busby), and EAR- 0711181 (to Busby). Many of the field relations described in this paper drew upon thesis geologic mapping supervised by Busby, including Steve DeOreo (MS), Noah Garrison (MS), Fabrice Roullet (MS), Carolyn Gorny (BS), Jeanette Hagan (PhD expected), and Alice Koerner (PhD expected). We thank the USGS EDMAP program for supporting some of this work, through award numbers 03HQAG0030, 05GQAG0010, and 06HQAG0061 (to Busby).

We thank the following people for valuable field discussions in the Sierra Nevada (while not holding them responsible for our interpretations): George Bergantz, Woody Brooks, Brian Cousens, Garniss Curtis, Jim Faulds, Larry Garside, Trobe Grose, Brian Hausback, Chris Henry, Angela Jayko, Nathan King, Christopher Pluhar, Dylan Rood, Jason Saleeby, Zorka Saleeby, George Saucedo, Ian Skilling, Burt Slemmons, Greg Stock, Jeff Tolhurst, David Wagner and John Wakabayashi. Office discussions with Pat Cashman, Richard Fisher, Cliff Hopson, Paul Renne and Rich Schweickert have also been valuable.

Comments from two anonymous reviewers on an earlier version of this manuscript, and reviews from Jason Saleeby and Jeanette Hagan, are kindly acknowledged. All of the 2006 – 2008 age data summarized in Table 1 were recalculated by Paul Renne (Berkeley Geochronology Center), and the 2009 data (Hagan et al., 2009) are his new dates; we are grateful to him for his careful attention to this matter. We thank Gerardo Torrez for his aid in geochemical analysis, and Jeanette Hagan for drawing figure 5.

CAPTIONS

Fig. 1- Tectonic setting of the Sierra Nevada. Shown are the locus of the Cretaceous Sierra Nevada batholith and its extension into northwest Nevada, and relicts of basins active during unroofing of the batholith in Late Cretaceous to Tertiary time (dot pattern). Positions of subduction-related magmatism in Cenozoic time are consistent with sea-floor evidence for subduction off California in Eocene and Oligocene time as summarized by Dickinson (2006) who interpreted the SSW-migrating magmatism to represent well-defined arc fronts that followed slab rollback. Sea-floor reconstruction at 15 Ma (Dickinson, 1997), showing positions of the triple junction at 15 Ma and 10 Ma. TJ1 marks the present position of triple junction between the San Andreas fault, the Cascadia subducton zone and the Mendocino fracture zone. The Sierran microplate lies between the San Andreas fault and the Walker Lane belt, which currently accommodates 20-25% of the plate motion between the North American and Pacific plates (see references in text),

and may represent the future plate boundary. This was born at 10 Ma within the Sierra Nevada Ancestral Cascades arc (Putirka and Busby, 2007) during high-K eruptions at the Little Walker caldera (L.W., Fig. 2).

Fig. 2 – Oligocene to Miocene paleogeography of part of the Basin and Range and Sierra Nevada,showing the position of the paleo- divide and Oligocene to Early Miocene calderas (Henry, 2008), and Tertiary paleochannels that funneled ignimbrites westward from the calderas in central Nevada to the Central Valley of California (Henry, 2008). Present-day Sierra Nevada range-front faults shown in blue. Note that paleo-channels are much better defined in the Sierra Nevada of California than they are in Nevada because they were not overprinted by prolonged subduction volcanism, nor were they disrupted by Basin and Range faults; this makes them ideal for reconstruction of landscape evolution. Progressive west-southwestward sweep of the Oligocene to Miocene arc front is shown, using data summarized by Cousens et al. (2008) and our new dates (Fig. 4). HL = Honey Lake, LT = Lake Tahoe, CP = Carson Pass, EP = Ebbetts Pass, SP = Sonora Pass, L.W. = 10 - 9 Ma Little Walker Caldera, ML = Mono Lake.

Fig. 3 – (A) Simplified cross-sectional view of low-angle subduction that created a high plateau across Nevada and eastern California in Cretaceous time, referred to as the Nevada-Plano (not drawn to scale) (De Celles, 2004). (B) Simple cartoon illustrating end-member models for Cenozoic landscape evolution (not to scale). Option 1: Block-faulting model for uplift of the Sierra Nevada at 3 – 6 Ma (Hamilton and Myers, 1966). Option 2: Origin of the Sierra Nevada on the shoulder of a high plateau inherited from Cretaceous time, disrupted by down-dropping of basins in Cenozoic time.

Fig. 4 – Distribution of our new $^{40}Ar/^{39}Ar$ dates on previously undated rocks of the Sierra Nevada Ancestral Cascades arc.

Fig. 5 – Distribution of Cenozoic volcanic rocks (dark gray), and faults along the central to northern Sierra Nevada – Basin and Range transition, with area shaded in light gray representing the Walker Lane belt. Brown dotted line represents the present-day Sierra

Nevada range crest. Brown circle represents the Little Walker Center/Caldera, described in text. Sources include Koenig, 1963; Stewart and Carlson, 1978; Wagner et al, 1981; Wagner and Saucedo, 1992; Henry and Perkins, 2001; Saucedo, 2005; Busby et al., 2008a, 2008b; Hagan et al., 2009; and Cashman et al., 2009. RCC-SR = Red Clover Creek-Stony Ridge sections of Garrison et al. (2008).

Fig. 6 – Outcrop photos of selected key features in the Sierra Nevada paleocanyons. (A) Unconformity 1, showing rugged paleo-relief carved into Mesozoic mesozonal granitic rock below; Tertiary volcanic-volcaniclastic rocks above. Photo taken on southeast side of Stanislaus Peak. (B) Sequence 1 weakly welded Oligocene ignimbrite, erupted from central Nevada; note small size of (flattened pumices), which is typical of these distal ignimbrites. (C) Unconformity 2, cut into sequence 1 Oligocene ignimbrites (not visible in photo) and overlain by Miocene andesitic volcaniclastic rocks with a basal lag of well-rounded granitic cobbles and boulders. Granitic clasts are very rare in the Miocene volcanic-volcaniclastic section, except along unconformities. (D) Sequence 2 avalanche blocks composed of block-and-ash-flow tuff (yellow), enclosed in debris flow deposits at Carson Spur (map unit Tfdf, interstratified fluvial and debris flow deposits, Fig. 2 of Busby et al., 2008a). The block-and-ash-flow tuff blocks were derived from a 15 Ma hornblende trachyandesite block-and-ash-flow tuff preserved at the modern Sierran crest, 8 km up-paleocanyon (Thaba1 of Hagan et al., 2009). (E) Petrified wood is common in debris flow deposits, and charred wood occurs in block-and-ash-flow tuffs of the paleocanyon fills; this example is from sequence 2. (F) Andesite block-and-ash-flow tuff, typical of sequences 2 through 4: they are massive, with monomict angular to subrounded blocks up to 1 m in diameter, set in an unsorted lapilli- to ash-sized matrix of the same composition. This photo comes from sequence 2 at Sonora Pass (Relief Peak Formation). (G) Interstratified andesitic debris flow and fluvial deposits, typical of sequences 2 through 4. Debris flow deposit are massive, unsorted, and contain a variety of andesite clast types supported in a pebbly sandstone matrix, whereas fluvial deposits are stratified and sorted, and show better rounding of clasts. These strata are tilted because they lie within a 1.6 km long avalanche block derived from sequence 2 by landsliding along a range-front fault immediately prior to eruption of sequence 3 high-K rocks at Sonora Pass.

(H) Fluvial boulder conglomerate typical of sequence 2, 3 and 4. Note imbrication. (I) Fluvial pebble and cobble conglomerate typical of sequences 2, 3 and 4. (J) Angular unconformity (unconformity 3) produced by siding of megablocks of sequence 2 strata onto the downthrown block of a range-front fault (tilted strata), within 140 kyr of the eruption of the overlying sequence 3 Table Mountain Latite lava flows from the Little Walker Center (overlying flat-lying strata). Unconformity 3 elsewhere consists of an erosional unconformity (see text). Photo taken on east side of Sonora Pass, looking south toward Sardine Falls (lower left). (K) Sequence 3 high-K lava flows of the Table Mountain Latite: trachyandesite and trachybasaltic andesite. In this flow, the columnar-jointed base passes upward into complexly blocky-jointed top typical of lava quenched by water running over it. This is consistent with its emplacement in a paleo-river canyon. Photo taken west of Sonora Pass in the Dardanelles area. (L) Stretched vesicles in the Table Mountain Latite, oriented parallel to the WSW-ENE-trending paleocanyon (Koerner et al., 2009). (M) Sequence 3 high-K ignimbrite of the Eureka Valley Tuff: trachydacite (Koerner et al., 2009). This outcrop passes upward from glassy, densely-welded ignimbrite into devitrifed, less densely-welded ignimbrite. (N) Closeup of Eureka Valley Tuff (sequence 3), showing typical black fiamme, and abundant light gray volcanic rock fragments. (O) Conglomerate overlying unconformity 4: Megaboulders of granitic basement encased in a cobble to boulder conglomerate with andesitic and granitic clasts. These clasts were funneled down a relay ramp between overlapping normal faults (see text). (P) Sequence 4 breccias, Ebbetts Pass: extremely coarse-grained deposits record rejuvenation and beheading of the paleocanyon system along range-front faults at about 7 Ma. (Q) Sequence 4 basalt lava flow, showing a well-developed a'a crust; other basalt flows in the section have pahoehoe crusts, but hornblende andesite block-and-ash-flow tiffs and lava flows dominate sequence 4 (Hagan et al. 2009). (R) Sequence 4 Ebbettts Pass Center, sited on the Grover Hot Spring fault (not visible): Strata on right side of photo consist of basaltic andesite lava flows that dip away from the center, with primary dip angle of about 30 degrees. Light gray rocks on the skyline at the left side of the photo are dacite intrusions that form the core of the center. Our unpublished mapping shows that basaltic andesite lava flows dip away from the silicic intrusive core to form a mafic shield with a radius of about 8 km. Field of view of photo is about 4 km.

Fig. 7 – Sketch model for the Cenozoic tectonic evolution of the central Sierra Nevada. Cartoon cross sections illustrate key features in the crust and subducting slab, and are not drawn to scale.

Table 1 – Summary of our $^{40}Ar/^{39}Ar$ age data on Cenozoic volcanic rocks in the central and northern Sierra Nevada.

REFERENCES

Armin, R.A., John, D.A., Moore, W.J., and Dohrenwend, J.C., 1984, Geologic Map of the Markleeville 15 Minute Quadrangle, Alpine County, California, Department of the Interior - United States Geologic Survey.

Bateman, P.C., and Wahrhaftig, C., 1966, Geology of the Sierra Nevada, in Bailey, E.H., ed., Geology of northern California, Volume 190: California Division of Mines Bulletin, p. 107-172.

Busby, C.J. and Bassett, K., 2007, Volcanic facies architecture of an intra-arc strike-slip basin, Santa Rita Mountains, Arizona: Bulletin of Volcanology, v. 70, no. 1, p. 85 – 103.

Argus, D.F., and R.G. Gordon, 1991, Current Sierra Nevada–North America motion from very long baseline interferometry: implications for the kinematics of the Western United States: Geology, v. 19, p. 1085–1088.

Armstrong, R.L., and Ward, P., 1991, Evolving geographic patterns of Cenozoic magatism in the North America Cordillera: The temporal and spatial association f magmatism and core complexes: Juornal of Geophysical Research, v. 96, p. 13,201-13,224.

Axen, G. J. , Taylor, W. J. , and Bartley, J. M. , 1993, Space-time patterns of the onset of extension and magmatism, southern Great Basin, Nevada, Utah and California: Geological Society of America Bulletin v. 105, p. 56-76 (doi:10.1130/0016-7606(1993)105<0056:STPATC>2.3.CO:2, 1993).

Bartow, J. A. , 1991, The Cenozoic evolution of the San Joaquin Valley, California: U.S. Geological Survey Professional Paper 1501, pp.

Bennett, R.A., Davis, J.L., and Wernicke, B.P., 1999, Present-day pattern of Cordilleran deformation in the western United States: Geology, v. 27, p. 371-374.

Busby, C., DeOreo, S., Skilling, I., Gans, P, and Hagan, J., 2008, Carson Pass-Kirkwood paleocanyon system: implications for the Tertiary evolution of the Sierra Nevada, California: Geological Society of America Bulletin, v. 120, no. 3/4, p. 274-299.

Busby, C.J., Hagan, J., Putirka, K., Pluhar, C., Gans, P., Rood, D., DeOeo, S., Skilling, I. and Wagner, D., 2008, The ancestral Cascades arc: Implicatons for the development of the Sierran microplate and tectonic significance of high K_2O volcanism: in, J. Wright and J. Shervais (eds), Ophiolites, Arcs and Batholiths: Geological Society of America Special Paper 438, p. 331-378.

Cashman, P.H., Trexler, J.H., Muntean, T.W., Faulds, J.E., Louie, J.N., and Oppliger, G., 2009, Neogene tectonic evolution of the Sierra Nevada – Basin and Range transition zone at the latitude of Carson City, Nevada:

Christensen, M.N., 1966, Late Cenozoic crustal movements in the Sierra Nevada of California: Geological Society of America Bulletin, v. 77, p.163–181.

Clark, M.K., Mahéo, G., Saleeby, J., and Farley, K.A., 2005, The non-equilibrium landscape of the southern Sierra Nevada, California: GSA Today, v. 15, p. 4-10.

Cecil, M.R., Ducea, M.N., Reiders, P.W., and Chase, C.G., 2007, Cenozoic exhumation of the northern Sierra Nevada, California, from (U-Th)/He thermochronology: Geological Society of America Bulletin.

Cousens, B., Prytulak, J., Henry, C., Alcazar, A. & Brownrigg, T., 2008, Geology, geochronology, and geochemistry of the Mio-Pliocene Ancestral Cascades arc, northern Sierra Nevada, California and Nevada: The roles of the upper mantle subducting slab, and the Sierra Nevada lithosphere: Geosphere**,** v. 4, p. 829-853.

DeCelles, P. G., 2004, Late Jurassic to Eocene evolution of the Cordilleran thrust belt and foreland basin system, western U.S.A.: American Journal of Science, v. 304, p. 105-168.

Dickinson, W. R., 1997, Tectonic Implications of Cenozoic volcanism in coastal California: Geological Society of America Bulletin, v. **109**, p. 936 – 934.

Dickinson, W. R. , 2006, Geotectonic evolution of the Great Basin: Geosphere, v. 2, no. 7, p. 353-368; doi: 10.1130/GES00054.1.

Dixon, T.H., Miller, M., Farina, F., Wang, H., and Johnson, D., 2000, Present-day motion of the Sierra Nevada block and some tectonic implications for the Basin and Range province, North American Cordillera: Tectonics, v. 19, p. 1-24.

Ducea MN, Saleeby JB. 1996. Buoyancy sources for a large, unrooted mountain range, the Sierra Nevada, California: Evidence from xenolith thermobarometry. Journal of Geophysical Research **101**: 8229–8244.

Ducea MN, Saleeby JB. 1998. A case for delamination of the deep batholithic crust beneath the Sierra Nevada. International Geology Review **40**: 78–93.

Flowers, R. M., D. L. Shuster, B. P. Wernicke, and K. A. Farley (2007), Radiation damage control on apatite (U-Th)/He dates from the Grand Canyon region, Colorado Plateau, Geology, 35(5), 447-450.

Gans, P. B. , Mahood, G. A., and Schermer, E. , 1989, Synextensional magmatism in the Basin and Rage province: a case study from the eastern Great Basin: Geological Society of America Special Paper 233, 53 pp.

Garrison, N., Busby, C.J., Gans, P.B., Putirka, K. and Wagner, D.L., 2008, A mantle plume beneath California? The mid-Miocene Lovejoy flood basalt, northern California: in, J. Wright and J. Shervais (eds), Ophiolites, Arcs and Batholiths: A Tribute to Cliff Hopson: Geological Society of America Special Paper 438, p. 551-572.

Garside, L.J., Henry, C.D., Faulds, J.E., and Hinz, N.H., 2005, The upper reaches of the Sierra Nevada auriferous gold channels, in Rhoden, H.N., ed., Window to the World, Geological Society of Nevada Symposium Proceedings, May 14 - 18, 2005.

Gorny, C., Busby, C., Pluhar, C., Hagan, J., and Putirka, K., 2009 this volume, An in-depth look at distal Sierra Nevada paleochannel fill: drill cores through the Table Mountain latite near Knight's Ferry: in review for the Nevadaplano special issue of International Geological Reviews, Gary Ernst, editor, 18 ms pp.

Grose, T.L.T., 2000a (preliminary), Geologic map of the Portola 15' Quadrangle, Plumas County, California: California Department of Conservation, Division of Mines and Geology Open File Report, scale 1:62,500.

Grose, T.L.T., 2000b (preliminary), with contributions from Durrell, C., and D'Allura, J.A., (preliminary), Geologic map of the Blairsden 15' Quadrangle, Plumas County, California: California Department of Conservation, Division of Mines and Geology Open File Report, scale 1:62,500.

Grose, T.L.T., 2000c (preliminary), Geologic map of the Loyalton 15' Quadrangle, Plumas and Sierra Counties, California: California Department of Conservation, Division of Mines and Geology Open File Report, scale 1:62,500.

Grose, T.L.T., 2000d (preliminary), Geologic map of the Sierraville 15' Quadrangle, Sierra and Plumas Counties, California: California Department of Conservation, Division of Mines and Geology Open File Report, scale 1:62,500

Grose, T.L.T., Wagner, D.L., Saucedo, G.J. and Medrano, M.D., 1989, Geologic map of the Doyle 15-minute quadrangle, Lassen and Plumas Counties, California: California Department of Conservation, Division of Mines and Geology Open-File Report 89-31, scale 1:62,500.

Grose, T.L.T., Saucedo, G.J. and Wagner, D.L., 1990, Geologic map of the Susanville Quadrangle, Lassen County, California: California Department of Conservation, Division of Mines and Geology Open-File Report 91-01, scale 1:100,000.

Grose, T.L.T., and Mergner, M., 2000, Geologic map of the Chilcoot 15' Quadrangle Lassen and Plumas Counties, California: California Department of Conservation, Division of Mines and Geology Open File Report, scale 1:62,500.

Hagan, J., Busby, C., Renne, P., and Putirka, K., 2009 this volume, Cenozoic evolution of paleochannels, Ancestral Cascades magmas, and range-front faults in the Kirkwood - Carson Pass - Markleeville region (Central Sierra Nevada): in, Gary Ernst, editor, The Rise and Fall of the Nevada Plano, International Geological Reviews.

Hamilton, W., and Myers, W.B., 1966, Cenozoic tectonics of the western United States: Reviews of Geophysics, v. 4, p. 509-549.

Henry, C.D. and Perkins, M.E., 2001, Sierra Nevada – Basin and Rnage transition near Reno, Nevada: Two-stage development at 12 and 3 Ma: Geology, v. 29, p. 719-722.

Henry, C. D., 2008, Ash-flow tuffs and paleovalleys in northeastern Nevada: Implications for Eocene paleogeography and extension in the Sevier hinterland, northern Great Basin: Geosphere, v. **4**, p. 1-35.

Horton, T.W., Sjostrom, D.J., Abruzzese, M.J., Poage, M.A., Waldbauer, J.R., Hren, M., Wooden, J., and Chamberlain, C.P., 2004, Spatial and temporal variation of Cenozoic surface elevation in the Great Basin and Sierra Nevada: American Journal of Science, v. 304, p. 862-888.

Horton, T.W., and Chamberlain, C.P. (2006) Stable isotopic evidence for Neogene surface downdrop in the central Basin and Range Province. GSA Bulletin, v. 118, p. 475-490.

House, M.A., Wernicke, B.P., and Farley, K.A., 1998, Dating topography of the Sierra Nevada, California, using apatite (U-Th)/He ages: Nature, v. 396, p. 66-69.

House, M.A., Wernicke, B.P., and Farley, K.A., 2001, Paleo-geomorphology of the Sierra Nevada, California, from (U-Th)/He ages in apatite: American Journal of Science, v. 301, p. 77-102.

Huber, N.K., 1981, Amount and timing of late Cenozoic uplift and tilt of the central Sierra Nevada, California—Evidence from the upper San Joaquin river basin: U.S. Geological Survey Professional Paper 1197, 28pp.

Jones, C.H., Farmer, G.L., and Unruh, J.R., 2004, Tectonics of Pliocene removal of lithosphere of the Sierra Nevada, California: Geological Society of America Bulletin, v. 116, p. 1408-1422.

Keith, W.J., Dohrenwend, J.C., Guisso, J.R., and John, D.A., 1982, Geologic map of the Carson-Iceberg and Leavitt Lake Roadless Areas, central Sierra Nevada, California., *in* Map, M.F.S., ed., Report MF-1416-A, U.S. Geological Survey.

Kent-Corson, M.L., Sherman, L.S., Mulch, A., and Chamberlain, C.P. (2006) Cenozoic topographic and climatic response to changing tectonic boundary conditions in Western North America. Earth and Planetary Science Letters, v. 252, p. 453-466. .

King, N.M., Hillhouse, J.W., Gromme, S., Hausback, B.P., and Pluhar, C.J., 2007. Stratigraphy, paleomagnetism, geochemistry, and anisotropy of magnetic susceptibility of the Miocene Stanislaus Group, central Sierra Nevada and

Sweetwater Mountains, California and Nevada, Geosphere, Vol. 3, no. 6, pp. 646-666.

Koerner, A., Busby, C., Pluhar, C. and Putirka, K., 2009 this volume, New evidence for alternating effusive and explosive eruptions from the type section of the Stanislaus Group in the “cataract” paloecanyon, central Sierra Nevada (CA): in, Gary Ernst, editor, The Rise and Fall of the Nevada Plano, International Geological Reviews.

Koenig, J.B., 1963, Geologic map of California: Walker Lake sheet: California Division of Mines and Geology, scale 1:250,000.

Lerch, D. W., Miller, E., McWilliams, M. & Colgan, J., 2008, Tectonic and magmatic evolution of the northwestern Basin and Range and its transition to unextended volcanic plateaus: Black Rock Range, Nevada. Geological Society of America Bulletin v. 120, p. 300-311.

Lindgren, W., 1911, The Tertiary Gravels of the Sierra Nevada of California: Washington D.C., United States Geological Survey, 222 pp.

Loomis, D.P., and D.W. Burbank, 1988, The stratigraphic evolution of the El Paso Basin, Southern California; implications for the Miocene development of the Garlock Fault and uplift of the Sierra Nevada: Geological Society of America Bulletin, v. 100, p. 12–28.

Mahéo, G., K.A. Farley, M.K. Clark, and D. Shuster, 2004, Cooling and Exhumation of the Sierra Nevada Batholith in the Mount Whitney Area (California) Based on (U-Th)/He Thermochronometry: American Geophysical Union, Abstract T41D-1252, San Francisco.

Mulch, A., Graham, S. A. , and Chamberlain, C. P. , 2006, Hydrogen isotopes in Eocene river gravels and paleoelevation of the Sierra Nevada: Science, v. 313, no. 87, p. 87–89.

Mulch, A., Teyssier, C., Cosca, M.A., and Chamberlain, C.P. (2007) Stable isotope paleoaltimetry of Eocene core complexes in the North American Cordillera. Tectonics, v. 26, doi:10.1029/2006TC001995

Mulch, A., Sarna-Wojcicki, A.M., Perkins, M.E., and Chamberlain, C.P., 2008, A Miocene to Pleaistocene climate and elevation record of the Sierra Nevada

(California): Proceedings of the National Academy of Science, v. 105(19), p. 6819-6824,

Noble, D.C., Slemmons, D.B., Korringa, M.K., Dickinson, W.R., Al-Rawi, Y., and McKee, E.H., 1974, Eureka Valley Tuff, east-central California and adjacent Nevada: Geology, v. 2, p. 139-142.

Noble, D.C., Korringa, M.K., Church, S.E., Bowman, H.R., Silberman, M.L., and Heropoulos, C., 1976, Elemental and isotopic geochemistry of nonhydrated quartz latite glasses from the Eureka Valley Tuff, East-central California: Geological Society of America Bulletin, v. 87, p. 754-762.

Oldow, J.S., 2000, Displacement transfer and differential block motion in the central Walker Lane, western Great Basin: Eos, Transactions, American Geophysical Union, v. 81, p. 1174.

Pelletier, J.D. Numerical modeling of the Cenozoic geomorphic evolution of the southern Sierra Nevada, California. Earth Planet Sci Lett. 2007;259:85–96.

Pluhar, C., Deino, A., King, N., Busby, C., Hausback, B., Wright, T., and Fischer, C., 2009 this volume, Magnetostratigraphy, geochronology and proposed revision of Stanislaus Group stratigraphy: in, Gary Ernst, editor, The Rise and Fall of the Nevada Plano, International Geological Reviews.

Poage, M.A., and Chamberlain, C.P. (2002) Stable isotopic evidence for a pre-Middle Miocene rainshadow in the western Basin and Range: implications for the surface uplift of the Sierra Nevada. Tectonics, v. 21, 16-1 - 16-10.

Priest, G.R., 1979, Geology and geochemistry of the Little Walker volcanic center, Mono County, California: unpublished PhD thesis, Oregon State University

Proffett, J. M., 1977, Cenozoic geology of the Yerington district, Nevada, and implications for the nature and origin of Basin and Range faulting: Geol. Soc. America Bull., v. 88, p. 247-266.

Putirka, K., and Busby, C.J., 2007, The tectonic significance of high K2O volcanism in the Sierra Nevada, California: Geology, V. 35, no. 10, p. 923 – 926.

Ransome, F.L., 1898, Some lava flows on the western slope of the Sierra Nevada, California, United States Geological Survey Bulletin, Volume 89, p. 71.

Saleeby, J., and Z. Foster, 2004, Topographic response to mantle lithosphere removal, southern Sierra Nevada region, California: Geology, v. 32, p. 245-248.

Saucedo, G.J., 2005, Geologic map of the Lake Tahoe basin, California and Nevada: Map no. 4, 1:100,000 Scale Regional Geologic Map Series, California Geological Survey.

Saucedo, G. J., and Wagner, D. L., 1992, Geologic Map of the Chico Quadrangle, 1:250,000: California Division of Mines and Geology Regional Map Series, v. 7A.

Sella, G.F., T.H. Dixon, and A. Mao, 2002, REVEL: a model for recent plate velocities from space geodesy: Journal of Geophysical Research, v. 107, 17 p.

Shuster, D. L., R. M. Flowers, and K. A. Farley (2006), The influence of natural radiation damage on helium diffusion kinetics in apatite, Earth Planet. Sci. Let., 249(3-4), 148-161.

Schweickert, R.A., Lahren, M.M., Smith, K.D., and Karlin, R.D., 1999, Preliminary map of active faults of the Lake Tahoe basin: Seismological Research Letters, v. 70, p. 306-312.

Schweickert, R.A., Lahren, M.M., Karlin, R.D., and Howle, J., 2000, Lake Tahoe active faults, landslides, and tsunamis, in Lageson, D.R., Peters, S.G., and Lahren, M.M., eds., Great Basin and Sierra Nevada: Boulder, Colorado, Geological Society of America Field Guide 2, p. 1-22.

Schweickert, R.A., Lahren, M.M., Smith, K.D., Howle, J.F., and Ichinose, G., 2004, Transtensional deformation in the Lake Tahoe region, California and Nevada, USA: Tectonophysics, v. 392, p. 303-323.

Skilling, I, Busby, C. and Imai, T., in review this volume, Mass wasting events triggered by Ancestral Cascades arc lava dome collapses in Miocene paleocanyons of the central Sierra Nevada (CA): Evidence for high relief: in, Gary Ernst, editor, The Rise and Fall of the Nevada Plano, International Geological Reviews.

Slemmons, D.B., 1953, Geology of the Sonora Pass region [PhD thesis]: Berkeley, University of California.

Slemmons, D.B., 1966, Cenozoic volcanism of the central Sierra Nevada, California, Geology of Northern California, Bulletin of the California Division of Mines and Geology, p. 199-208.

Smith, G. A., and Lowe, D. R. , 1991, Lahars: volcano-hydrologic events and deposition in the debris flow – hyperconcentrated flood flow continuum. In, R.V. Fisher and G.A. Smith (eds) Sedimentation in volcanic settings: SEMP Special Publication 45, p. 59-70.

Stewart, J.H., and Carlson, J.E., 1978, Geologic map of Nevada: U.S. Geological Survey in collaboration with Nevada Bureau of Mines and Geology, scale 1:500,000.

Stock, G.M., Anderson, R.S., and Finkel, R.C., 2004, Pace of landscape evolution in the Sierra Nevada, California, revealed by cosmogenic dating of cave sediments: Geology, v. 32, p. 193-196.

Stock, G.M., Anderson, R.S., and Finkel, R.C., 2005, Rates of erosion and topographic evolution of the Sierra Nevada, California, inferred from cosmogenic 26Al and 10Be concentrations: Earth Surface Processes Landforms., v. 30, p. 985–1006.

Stockli, D.F., Surpless, B.E. and Dumitru, T.A., 2002, Thermochronological constraints on the timing and magnitude of Miocene and Pliocene extension in the central Wassuk Range, western Nevada: Tectonics, v. 21, no. 4, p. 10-1 – 10-19.

Surpless, B.E., Stockli, D.F., Dumitru, T.A., and Miller, E.L., 2002, Two-phase westward encroachment of Basin and Range extension into the northern Sierra Nevada: Tectonics, v. 21, p. 1002.

Thatcher, W., Foulger, G.R., Julian, B.R., Svarc, J.L., Quily, E., and Bawden, G.W., 1999, Present-day deformation across the Basin and Range Province, Western United States: Science, v. 283, p. 1714-1718.

Unruh, J.R., 1991, The uplift of the Sierra Nevada and implications for late Cenozoic epeirogeny in the western Cordillera: Geological Society of America Bulletin, v. 103, p. 1395–1404.

Unruh, J.R., Humphrey, J., and Barron, A., 2003, Transtensional model for the Sierra Nevada frontal fault system, eastern California: Geology, v. 31, p. 327-330.

Wakabayashi, J., and Sawyer, T.L., 2001, Stream Incision, Tectonics, Uplift, and Evolution of Topography of the Sierra Nevada, California: The Journal of Geology, v. 109, p. 539-562.

Wagner, D.L., Jennings, C.W., Bedrossian, T.L., and Bortugno, E.J., 1981, Geologic map of the Sacramento quadrangle, California, 1:250,000: California Division of Mines and Geology, Regional Geologic Map 1A, scale 1:250,000.

Whitney, J.D., 1880, Harvard University, Museum of Comparative Zoology, Memoirs, v. 1, p. 659.

Wolfe, J.A., Schorn, H.E., Forest, C.E., and Molnar, P., 1997, Paleobotanical Evidence for High Altitudes in Nevada During the Miocene: Science, v. 276, p. 1672-1675.

Zandt, G., H. Gilbert, T. Owens, M. Ducea, J. Saleeby, and C. Jones, 2004, Active foundering of a continental arc root beneath the southern Sierra Nevada, California: Nature, v. 43, p. 41-45.

.

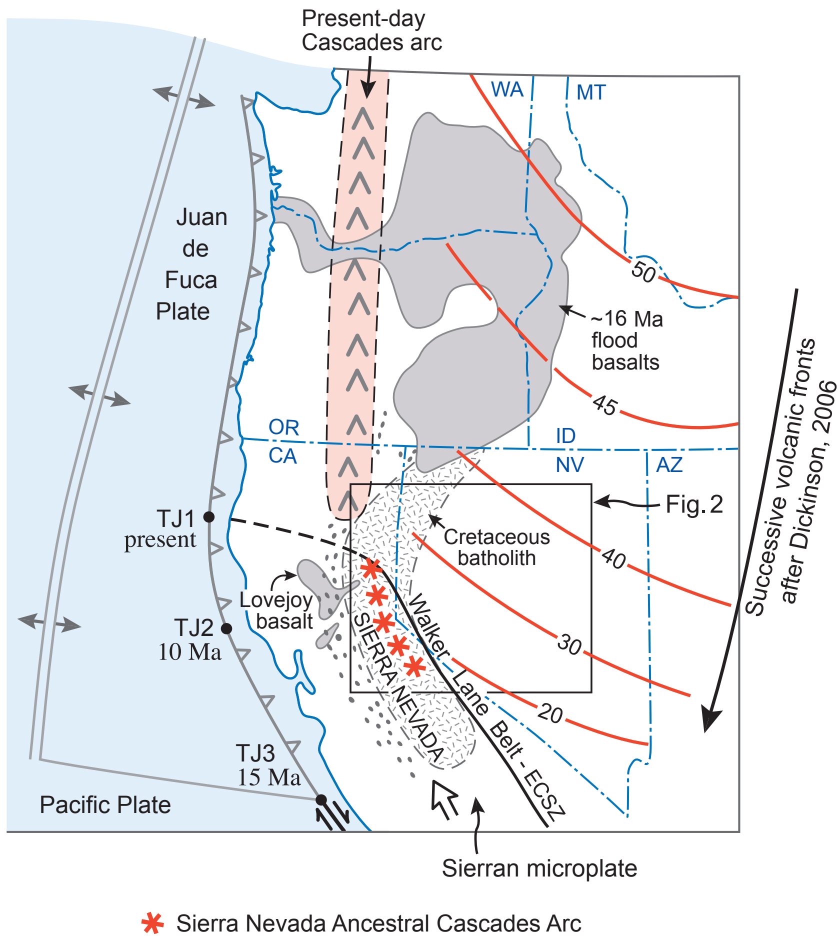
Present-day
Cascades arc
WA
MT
Juan
de
Fuca
Plate
50
~16 Ma
flood
basalts
45
OR
CA
ID
NV
AZ
Fig. 2
TJ1
present
Cretaceous
batholith
40
Lovejoy
basalt
TJ2
10 Ma
30
Walker Lane Belt - ECSZ
SIERRA NEVADA
20
TJ3
15 Ma
Pacific Plate
Sierran microplate
Successive volcanic fronts
after Dickinson, 2006
Sierra Nevada Ancestral Cascades Arc

Fig. 1

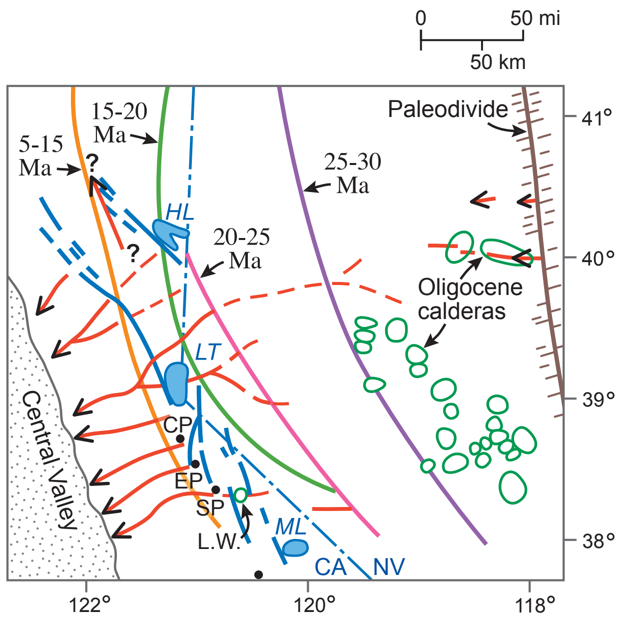
0
50 mi
50 km
Paleodivide
15-20
Ma
5-15
Ma
?
?
25-30
Ma
HL
20-25
Ma
Oligocene
calderas
LT
Central Valley
CP
EP
SP
L.W.
ML
CA
NV
41°
40°
39°
38°
122°
120°
118°

Fig. 2

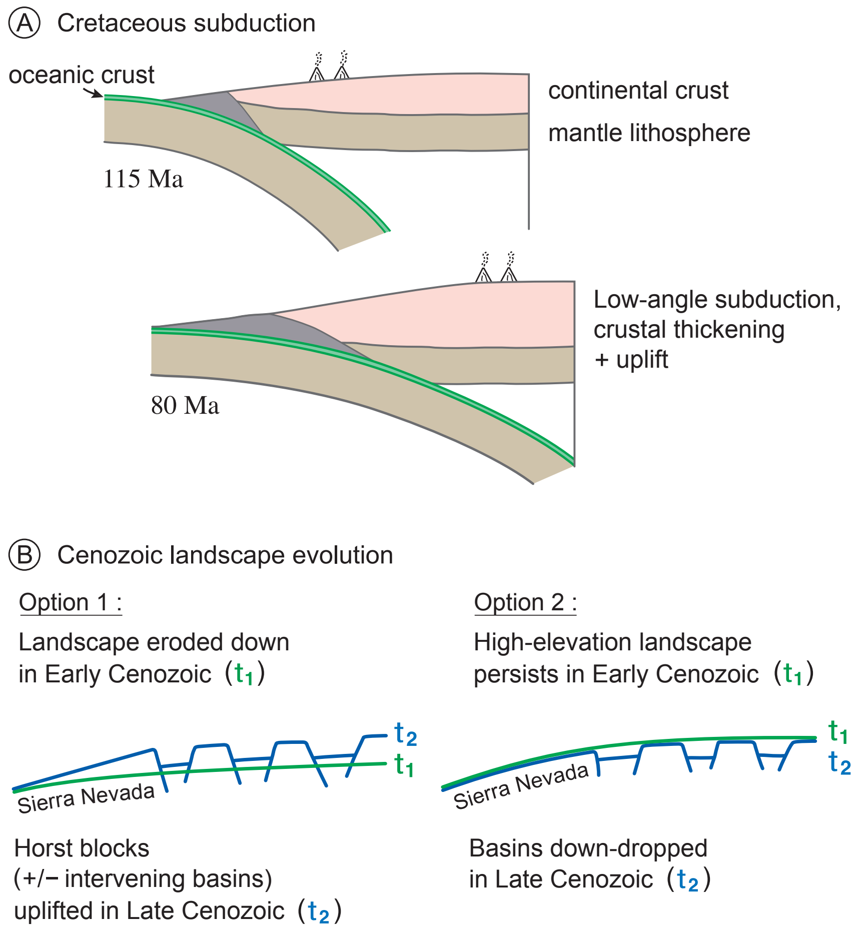
A Cretaceous subduction
oceanic crust
continental crust
mantle lithosphere
115 Ma
Low-angle subduction,
crustal thickening
+ uplift
80 Ma
B Cenozoic landscape evolution
Option 1 :
Landscape eroded down
in Early Cenozoic (t1)
t2
t1
Sierra Nevada
Horst blocks
(+/− intervening basins)
uplifted in Late Cenozoic (t2)
Option 2 :
High-elevation landscape
persists in Early Cenozoic (t1)
t1
t2
Sierra Nevada
Basins down-dropped
in Late Cenozoic (t2)

Fig. 3

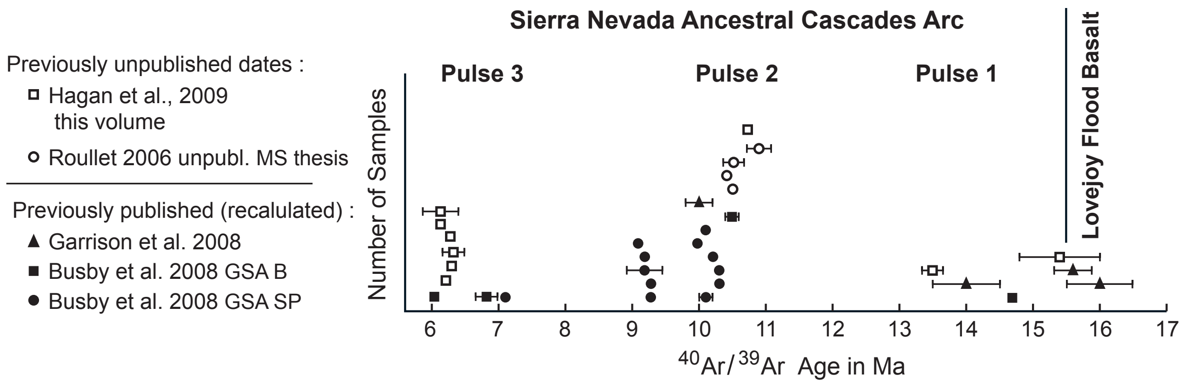
Sierra Nevada Ancestral Cascades Arc
Previously unpublished dates :
Hagan et al., 2009 this volume
Roullet 2006 unpubl. MS thesis
Previously published (recalulated) :
Garrison et al. 2008
Busby et al. 2008 GSA B
Busby et al. 2008 GSA SP
Pulse 3
Pulse 2
Pulse 1
Lovejoy Flood Basalt
Number of Samples
6 7 8 9 10 11 12 13 14 15 16 17
$^{40}Ar/^{39}Ar$ Age in Ma

Fig. 4

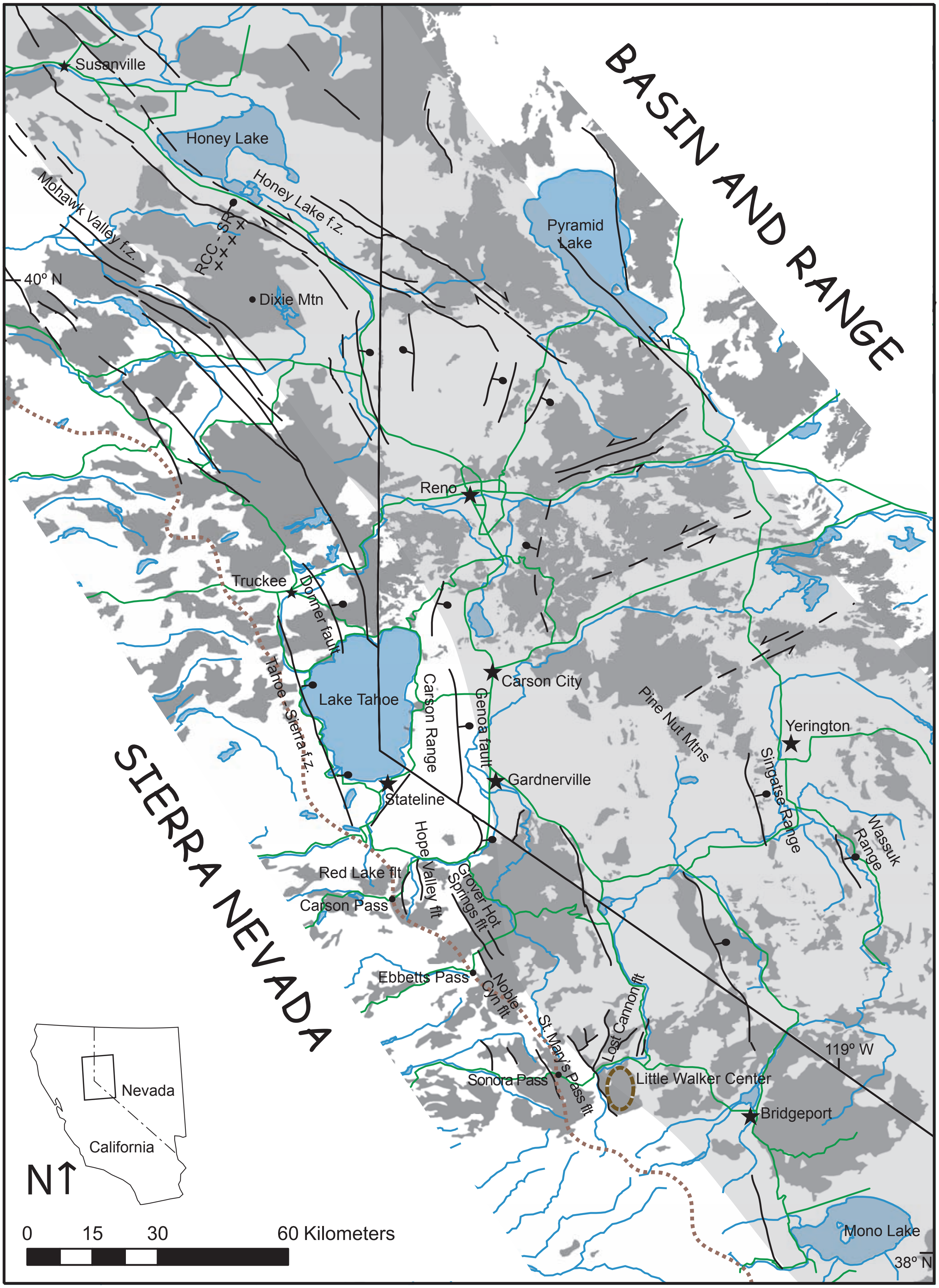
BASIN AND RANGE
SIERRA NEVADA
Susanville
Honey Lake
Honey Lake f.z.
Mohawk Valley f.z.
RCC - SR
Pyramid Lake
40° N
Dixie Mtn
Reno
Truckee
Donner fault
Lake Tahoe
Tahoe - Sierra f.z.
Carson Range
Genoa fault
Carson City
Pine Nut Mtns
Yerington
Singatse Range
Wassuk Range
Gardnerville
Stateline
Hope Valley flt
Grover Hot Springs flt
Red Lake flt
Carson Pass
Ebbetts Pass
Noble Cyn flt
St. Mary's Pass flt
Lost Cannon flt
Sonora Pass
Little Walker Center
119° W
Bridgeport
Mono Lake
38° N
Nevada
California
N
0
15
30
60 Kilometers

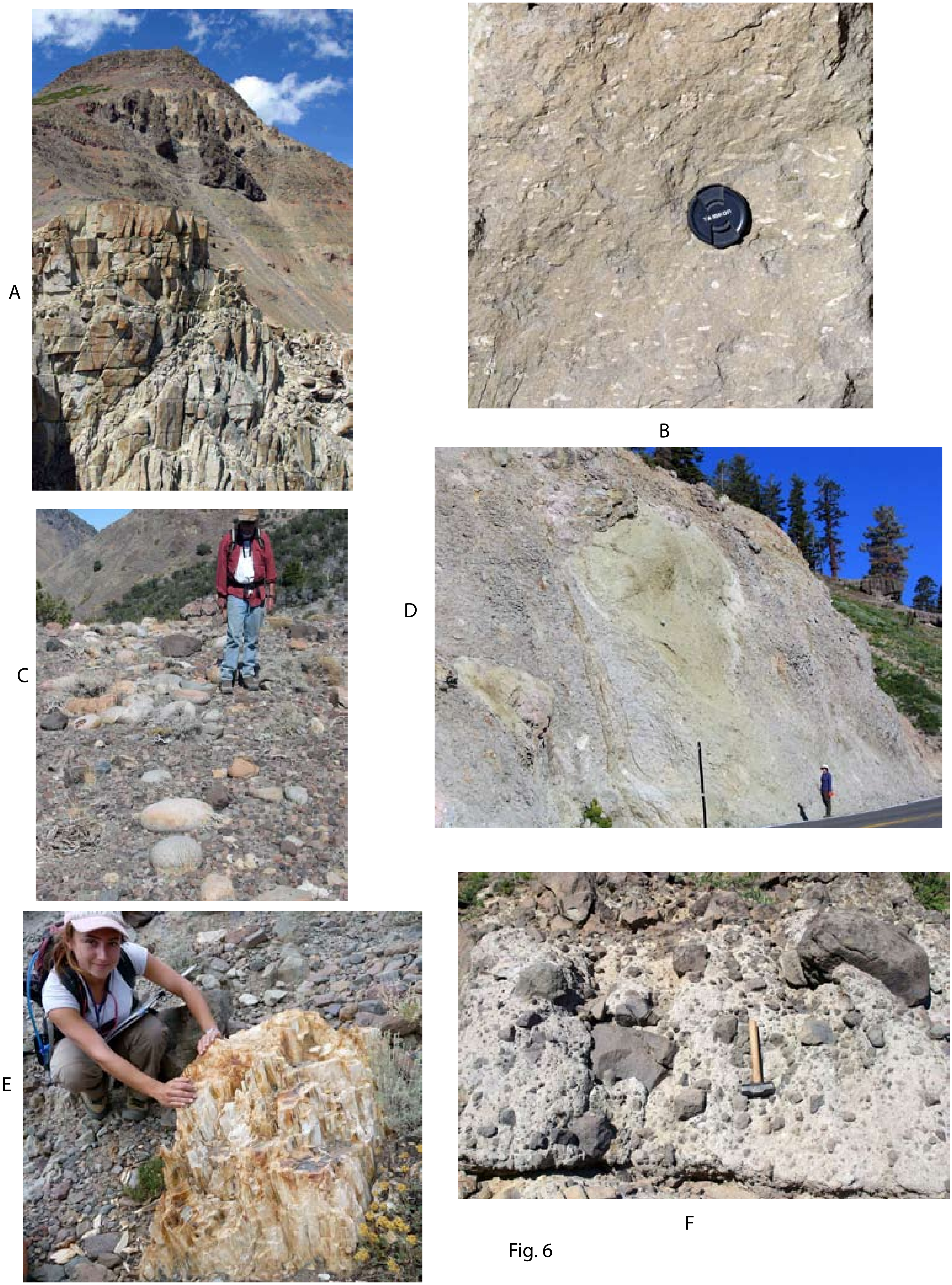

Fig. 6

G

H

I

J

K

L

Fig. 6, cont'd

M

N

O

P

Q

R

Fig. 6, cont'd

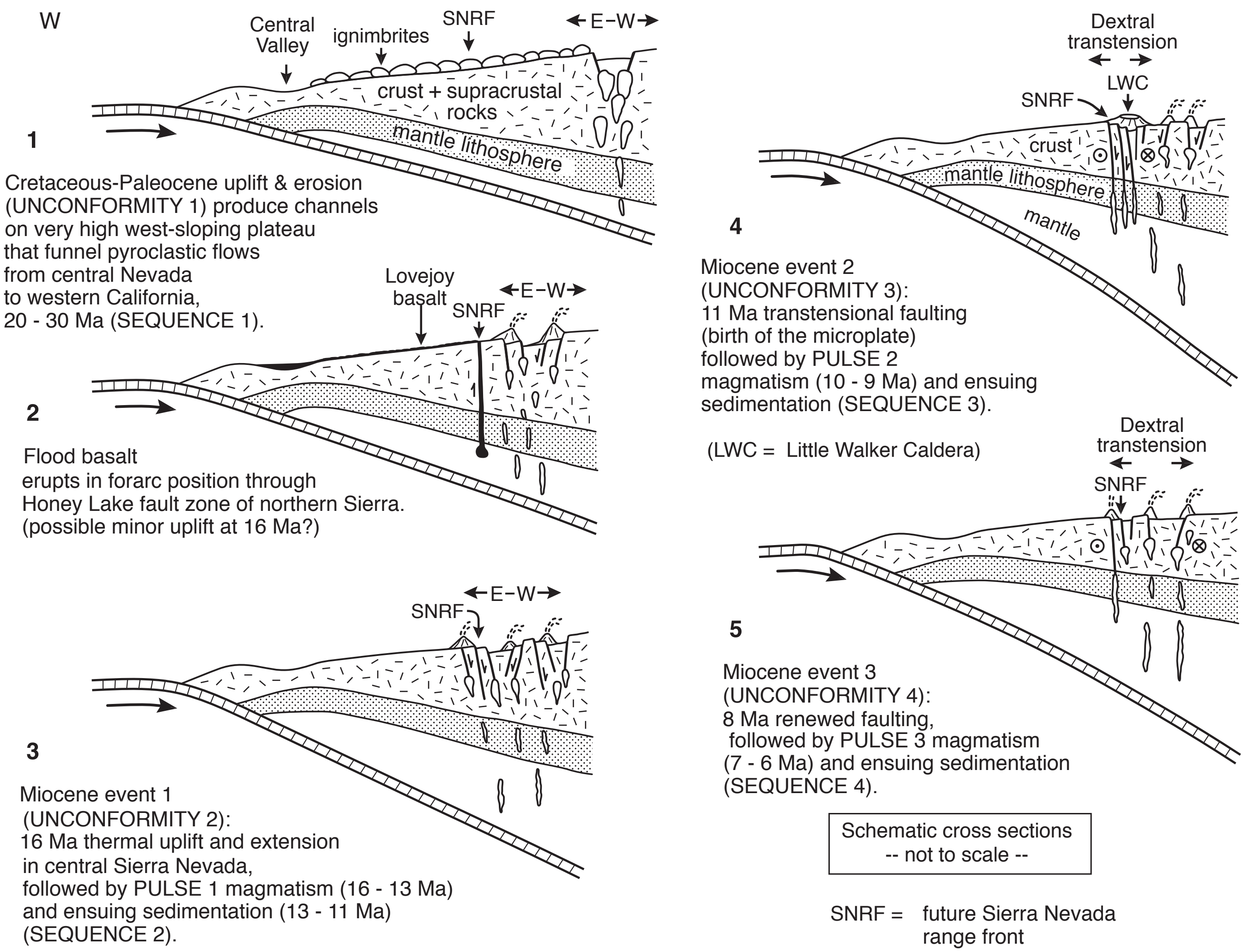
W
Central Valley
ignimbrites
SNRF
E–W
crust + supracrustal rocks
mantle lithosphere
1
Cretaceous-Paleocene uplift & erosion (UNCONFORMITY 1) produce channels on very high west-sloping plateau that funnel pyroclastic flows from central Nevada to western California, 20 - 30 Ma (SEQUENCE 1).
Lovejoy basalt
SNRF
E–W
2
Flood basalt erupts in forarc position through Honey Lake fault zone of northern Sierra. (possible minor uplift at 16 Ma?)
E–W
SNRF
3
Miocene event 1 (UNCONFORMITY 2): 16 Ma thermal uplift and extension in central Sierra Nevada, followed by PULSE 1 magmatism (16 - 13 Ma) and ensuing sedimentation (13 - 11 Ma) (SEQUENCE 2).
Dextral transtension
LWC
SNRF
crust
mantle lithosphere
mantle
4
Miocene event 2 (UNCONFORMITY 3): 11 Ma transtensional faulting (birth of the microplate) followed by PULSE 2 magmatism (10 - 9 Ma) and ensuing sedimentation (SEQUENCE 3).
(LWC = Little Walker Caldera)
Dextral transtension
SNRF
5
Miocene event 3 (UNCONFORMITY 4): 8 Ma renewed faulting, followed by PULSE 3 magmatism (7 - 6 Ma) and ensuing sedimentation (SEQUENCE 4).
Schematic cross sections -- not to scale --
SNRF = future Sierra Nevada range front

Fig. 7

A - Sonora Pass (Busby et al., 2008b)											
					Interpreted Age (Ma)[0]		Nominal Age (Ma)[1]		**Preferred Age (Ma)[2]**		
Sample #	Geochem	Mineral	Lat (°N)	Long (°W)	Age	± 2s	Age	± 2s	**Age**	**± 2s**	Unit Name
BP068	andesite	Hbl	38.37609	119.76975	7.12	0.06	7.22	0.06	**7.28**	**0.06**	Hbl Andesite Plug - Disaster Peak FM
BP068	andesite	Plag	38.37609	119.76975	7.0	0.5	7.11	0.5	**7.15**	**0.5**	Hbl Andesite Plug - Disaster Peak FM
TF003	trachydacite	Plag	38.43096	119.44792	9.14	0.04	9.28	0.04	**9.34**	**0.04**	Upper Member, Eureka Valley Tuff - Stanislaus Gp
TF003	trachydacite	Bio	38.43096	119.44793	9.18	0.04	9.32	0.04	**9.38**	**0.04**	Upper Member, Eureka Valley Tuff - Stanislaus Gp
TF005b	trachydacite	Plag	38.43041	119.44805	9.2	0.3	9.34	0.3	**9.4**	**0.3**	By-Day Member, Eureka Valley Tuff - Stanislaus Gp
TF009	trachydacite	Plag	38.42891	119.44841	9.27	0.04	9.41	0.04	**9.47**	**0.04**	Tollhouse Flat Member, Eureka Valley Tuff - Stanislaus Gp
TF009	trachydacite	Bio	38.42891	119.44842	9.34	0.04	9.48	0.04	**9.54**	**0.04**	Tollhouse Flat Member, Eureka Valley Tuff - Stanislaus Gp
PC032	shoshonite	Plag	38.35378	119.6344	10.14	0.06	10.30	0.06	**10.36**	**0.06**	Uppermost Table Mtn Latite Flow - Stanislaus Gp
PC005	trachyandesite	Plag	38.34641	119.63263	10.19	0.08	10.35	0.08	**10.41**	**0.08**	Lowermost Table Mtn Latite Flow - Stanislaus Gp
PC-AD	andesite	WR	38.34641	119.63265	10.35	0.25	10.51	0.25	**10.58**	**0.25**	Andesite dike - Upper Relief Peak Fm
PC-BA	bas andesite	Hbl	38.34427	119.6340	10.17	0.18	10.33	0.18	**10.39**	**0.18**	Block-and-ash flow tuff - Upper Relief Peak Fm
PC-BA	bas andesite	Plag	38.34427	119.6341	~10	na	~10	na	**~10**	**na**	Block-and-ash flow tuff - Upper Relief Peak Fm
BP057	-	Plag	38.37824	119.7430	23.8	0.2	24.16	0.2	**24.32**	**0.2**	Uppermost welded ignimbrite - Valley Springs Fm

B - Carson Pass - Kirkwood (Busby et al., 2008a)												
					Interpreted Age (Ma)[0]		Nominal Age (Ma)[1]		**Preferred Age (Ma)[2]**			
Sample #	Geochem	Mineral	Lat (°N)	Long (°W)	Age	± 2s	Age	± 2s	**Age**	**± 2s**	Unit Name	Map Unit
SBDCP61	andesite	Plag	38.6979	120.0888	6.05	0.12	6.14	0.12	**6.18**	**0.12**	Sentinels block-and-ash-flow tuff	Taba3
SBDCP62	basalt	WR	38.7101	120.0187	6.80	0.20	6.90	0.20	**6.95**	**0.20**	Basalt lava flow	Tbl
SBDCP20	andesite	Plag	38.6855	120.0617	10.49	0.12	10.65	0.12	**10.72**	**0.12**	Peperitic andesite dike in debris flow deposit	Tvdf1
SBDCP30	trachyandesite	Bio	38.7014	120.0003	14.69	0.06	14.91	0.06	**15.01**	**0.06**	Carson Pass hornblende trachyandesite block-and-ash-flow tuff	Thaba1

C - Hope Valley - Carson Pass (Hagan et al., 2009)												
					Interpreted Age (Ma)[0]		Nominal Age (Ma)[1]		**Preferred Age (Ma)[2]**			
Sample #	Geochem	Mineral	Lat (°N)	Long (°W)			Age	± 2s	**Age**	**± 2s**	Unit Name	Map Unit
ERLPk	bas.andesite	Hbl	38.7158	119.9857	na		6.09	0.34	**6.13**	**0.34**	Red Lake Pk pyroxene basaltic andesite block-and-ash-flow tuff	Tpaba
JHCP-67	andesite	Hbl	38.6600	119.8996	na		6.14	0.14	**6.18**	**0.14**	Markleeville Pk hb-bt dacite and andesite intrusions	Thbdi
JHCP-56	andesite	Hbl	38.6909	119.9799	na		6.18	0.14	**6.22**	**0.14**	Lower hornblende andesite lava flow	Thalu
JHCP-13	bas. andesite	Hbl	38.7122	119.9856	na		6.25	0.10	**6.29**	**0.10**	Red Lake Pk pyroxene basaltic andesite block-and-ash-flow tuff	Tpaba
JHCP-53	dacite	Hbl	38.6581	119.9233	na		6.30	0.14	**6.34**	**0.14**	Markleeville Pk hb-bt dacite and andesite intrusions	Thbdi
JHCP-69	andesite	Hbl	38.6644	119.8947	na		6.33	0.24	**6.37**	**0.24**	Hornblende andesite dike of Markleeville Pk	Thadp
JHCP-44	andesite	Hbl	38.7544	119.8969	na		10.70	0.10	**10.77**	**0.10**	Pyroxene andesite intrusion of Pickett Pk	Tpai
JHCP-14	andesite	Hbl	38.7184	119.9853	na		13.51	0.16	**13.61**	**0.16**	Red Lake Pk hb andesite block-and-ash-flow tuff	Thaba2
JHCP-7	andesite	Plag	38.6433	119.9037	na		15.4	0.6	**15.5**	**0.6**	Jeff Davis Pk pyx-hb andesite and dacite block-and-ash-flow tuff	Tphaba

D - Northern Sierra: Lovejoy basalt and overlying strata at Red Clover Creek (Garrison et al., 2008)												
					Interpreted Age (Ma)[0]		Nominal Age (Ma)[1]		**Preferred Age (Ma)[2]**			
Sample #	Geochem	Mineral	Lat (°N)	Long (°W)	Age	± 2s	Age	± 2s	**Age**	**± 2s**	Unit Name	Map Unit
02BrRCC10a	andesite	Plag	39.98858	120.5426	9.96	0.24	10.11	0.24	**10.18**	**0.24**	Hornblende andesiteblock-and-ash-flow tuff	Mhab
02BrRCC6	andesite	WR	39.9822	120.5480	14.00	0.50	14.21	0.50	**14.31**	**0.50**	Plagioclase andesite breccia	Mpb
03LJSR13	basalt	Plag	40.15567	120.48922	15.12	4.64	15.35	4.64	**15.45**	**4.64**	Proximal Lovejoy basalt (Stony Ridge) uppermost flow	
02LJRCC8-B	basalt	Plag	3998818	120.56505	15.30	2.58	15.53	2.58	**15.63**	**2.58**	Proximal Lovejoy basalt (Red Clover Creek) uppermost flow	Mlb
02LJRCC8-A	basalt	Plag	39.98818	120.56505	15.60	1.00	15.84	1.00	**15.94**	**1.00**	Proximal Lovejoy basalt (Red Clover Creek) uppermost flow	Mlb
03LJSTM3	basalt	WR	39.55137	121.57967	15.63	0.30	15.87	0.30	**15.97**	**0.30**	Distal coarse-grained Lovejoy basalt flow at South Table Mtn	
03LJSTM4	basalt	WR	39.5498	121.57642	16.00	0.50	16.24	0.50	**16.35**	**0.50**	Distal coarse-grained uppermost flow South Table Mtn	

E - Northern Sierra: Dixie Mountain Center (Roullet, 2006)												
					Interpreted Age (Ma)[0]		Nominal Age (Ma)[1]		**Preferred Age (Ma)[2]**			
Sample #	Geochem	Mineral	Lat (°N)	Long (°W)	**Age**	± 2s	**Age**	± 2s	**Age**	**± 2s**	Unit Name	Map Unit
Dixie 90	andesite	Plag	39.8559	120.33225	10.4	0.2	10.58	0.2	**10.65**	**0.2**	Hbl pyroxene andesite sill	Tuhpa
Dixie 2	andesite	Plag	39.54081	120.17758	10.50	0.20	10.66	0.20	**10.73**	**0.20**	Hbl biotite andesite intrusions	Thbai
Dixie 245	andesite	Plag	39.9372	120.3357	10.50	0.30	10.66	0.30	**10.73**	**0.30**	Block-and-ash-flow tuff	Tbaf2
Dixie 47b	andesite	Plag	39.54721	120.17793	10.85	0.20	11.02	0.20	**11.09**	**0.20**	Block-and-ash-flow tuff	Tbaf1

Notes:

[0]Interpreted age is calculated using 27.60 Ma for the FCs standard as reported by Gans in Busby et al., 2008a, 2008b; Garrison et al., 2008; and Roullet, 2006

[1]Nominal age is calculated using 28.02 Ma for the FCs standard (Renne et al., 1998)

[2]Preferred age is calculated using 28.201 Ma for the FCs standard (Kuiper et al., 2008)